ANL-FRA-167

Integrated Intra-subassembly Treatment in the SASSYS-1 LMR Systems Analysis Code

by Floyd Dunn

Argonne National Laboratory, Argonne, Illinois 60439
operated by The University of Chicago
for the United States Department of Energy under Contract W-31-109-Eng-38

DISCLAIMER

Reproduced from the best available copy.

Available to DOE and DOE contractors from the
Office of Scientific and Technical Information
P.O. Box 62
Oak Ridge, TN 37831
Prices available from (615) 576-8401

Available to the public from the
National Technical Information Service
U.S. Department of Commerce
5285 Port Royal Road
Springfield, VA 22161

ANL-FRA-167

ARGONNE NATIONAL LABORATORY
9700 South Cass Avenue
Argonne, IL 60439-4801

INTEGRATED INTRA-SUBASSEMBLY TREATMENT IN THE SASSYS-1 LMR SYSTEMS ANALYSIS CODE

by

Floyd Dunn

Reactor Analysis Division

November 1992

Work supported by
U.S. Department of Energy
Nuclear Energy Programs

THIS PAGE

WAS INTENTIONALLY

LEFT BLANK

Table of Contents

List of Figures

List of Tables

THIS PAGE

WAS INTENTIONALLY

LEFT BLANK

INTEGRATED INTRA-SUBASSEMBLY TREATMENT IN THE SASSYS-1 LMR SYSTEMS ANALYSIS CODE

by Floyd Dunn

ABSTRACT

A hot channel treatment has been added to the SASSYS-1 LMR systems analysis code by providing for a multiple pin treatment of each of one or more subassemblies. This is an explicit calculation of intra-subassembly effects, not a hot-channel adjustment to a calculated average channel. Thus, the code can account for effects such as transient flow redistribution, both within a subassembly and among subassemblies. The code now provides a total integrated thermal hydraulic treatment including a multiple pin treatment within subassemblies, a multi-channel treatment of the whole core, and models for the primary coolant loops, the intermediate coolant loops, the steam generators, and the balance of plant. Currently the multiple-pin option is only implemented for single-phase calculations. It is not applicable after the onset of boiling or pin disruption. The new multiple pin treatment is being verified with detailed temperature data from instrumented subassemblies in EBR-II, both steady-state and transient, with special emphasis on passive safety tests such as SHRT-45. For the SHRT-45 test, excellent agreement is obtained between code predictions and experimental measurements of coolant temperatures.

1.0 INTRODUCTION

The SASSYS-1 code[1] is an integrated LMR (Liquid Metal Reactor) systems analysis code. It includes a point kinetics treatment for core neutronics and reactivity feedback. It also includes a thermal hydraulic treatment of the core, the primary coolant system, and the intermediate coolant loops, coupled to a steam generator model[2] and a balance-of-plant model[3,4]. In addition, the code contains a control system model[5]. The SASSYS-1 code can handle any LMR design, loop or pool, with an arbitrary arrangement of components. The code is capable of analyzing a wide range of transients, from mild operational transients through more severe transients leading to sodium boiling in the core and possible melting of cladding and fuel. The main applications of the code have been in the analysis of passive safety and the analysis of shut-down heat removal.

SASSYS-1 uses a multi-channel treatment to represent the reactor core. A channel models one pin, its associated coolant, and a structure which represents the wrapper wire and/or the subassembly duct wall. The whole length of the subassembly from coolant inlet to coolant outlet is modeled, including the pin section and reflector regions above and below the pins. The pin section includes the core and the axial blankets, as well as a gas plenum region. An axial mesh is used for a channel. At each axial node one coolant temperature is calculated. Also at each axial node two radial temperature nodes are used for the structure and a number of radial nodes are used for the pin or the axial reflector. Previously, SASSYS-1 used one channel to represent a subassembly or a group of similar subassemblies. The multi-channel treatment provided a means to represent different subassemblies with different power levels, flow rates, and fuel burn-ups. Usually an average pin was modelled for each group of subassemblies. Thus, detailed average temperatures were calculated for various subassemblies, but peaking within a subassembly was not calculated.

The new multiple pin treatment was added to the code to account for pin-to-pin variations within a subassembly. This new multiple pin treatment can be used in at least two different ways. One approach is to use the new treatment to compute nominal or "best estimate" variations within a subassemblies. Another approach is to compute hot channel behavior due

to postulated deviations in coolant flow rate, coolant flow area, and pin power. When doing a whole-core analysis, one probably would not want the hot channel temperatures used in the reactivity feedback calculation or in the core outlet temperatures that feed into the primary loop calculations. Therefore, one would probably use parallel treatments for the same subassembly: a nominal one-pin or multi-pin treatment used for reactivity feedback, plus a hot channel treatment decoupled from the reactivity feedback and from the primary loop calculation. The hot channel treatment would be de-coupled by setting reactivity feedback coefficients to zero and by setting the number of subassemblies represented by this treatment to zero.

The multiple pin model is described in detail in Section 2 of this report. Section 3 contains the multiple pin analysis of the EBR-II SHRT-45 test. In addition to providing experimental validation for the new model, the SHRT-45 analysis in this section provides a detailed description of how the new multiple pin model can be used. Appendix A contains short descriptions of the new subroutines added to the code for this model, as well as existing routines that were modified. The new input required to run the multiple pin model is described in Appendix B.

2.0 MULTIPLE PIN MODEL DESCRIPTION

The new multiple pin treatment allows a number of coupled channels to be used to model a single subassembly. Thus a channel can represent a part of a subassembly instead of the whole subassembly. Peaking factors can be mechanistically calculated by reducing coolant flow areas and flow rates or increasing pin power levels in some channels.

2.1 Physical Model

In the new multiple pin option, the regions above and below the pin section of a subassembly are still represented by a single channel; but up to nine channels can be used to represent the pin section. Each channel in the pin section can represent one or more concentric rows of pins and their associated coolant. It is also possible for channels to represent slices of pins for a subassembly with a strong lateral power skew or for one with a hot subassembly on

one side and a cool subassembly on the opposite side. Figure 1 illustrates one way that a number of channels can be used to model the pin section of a subassembly as concentric rings of pins and coolant subchannels. The thimble flow region in this figure is a feature of the EBR-II XX09 instrumented subassembly and is not found in ordinary subassemblies. This case concentrates on the coolant subchannels and splits the pins. It is also possible to shift the channel boundaries half a pin and use a pin-based representation with intact pins and split coolant subchannels.

The new option accounts for coolant-to-coolant heat transfer between adjacent channels, including the effects of both conduction and turbulent mixing. It also accounts for subassembly-to-subassembly heat transfer from the duct wall of a subassembly, through the interstitial sodium, to the duct wall of a neighboring subassembly. In addition, axial conduction in the coolant is accounted for.

Figure 2 illustrates the axial representation of the subassembly flow, with parallel flow paths through the pin section. Each channel used to represent the pin section of a subassembly has its own separate time-dependent flow rate, and the flow rates in all channels in a subassembly are driven by common pressures at the inlet and outlet of the pin section. Thus, transient flow redistribution among channels is accounted for. The single flow rate in the regions above and below the pin section is the sum of the pin section flow rates, so the subassembly flow orifice sees the correct total flow rate. Even though the coolant-to-coolant heat transfer coefficient includes a term for turbulent mixing between coolant subchannels, one effect that the flow calculation does not account for is mass flow between channels in the pin section, although cross-flow at the ends of the pin section is allowed. Therefore, if recirculation loops occur within a subassembly at low flows, the model would calculate them; but the recirculation loops would go to the ends of the pin section.

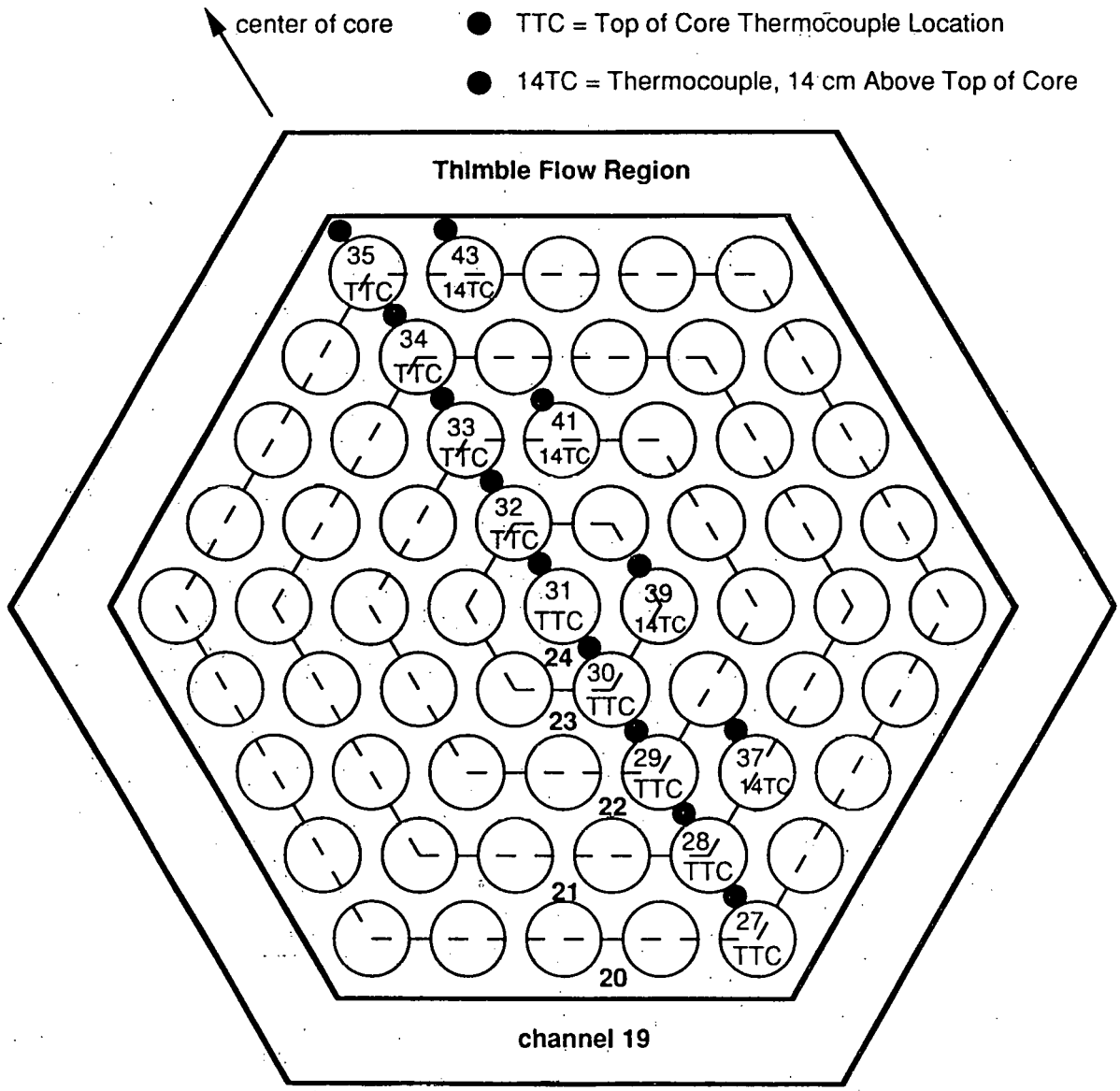

Figure 1. SASSYS-1 Multi-Channel Representation and Thermocouple Locations for the EBR-II XX09 Instrumented Subassembly

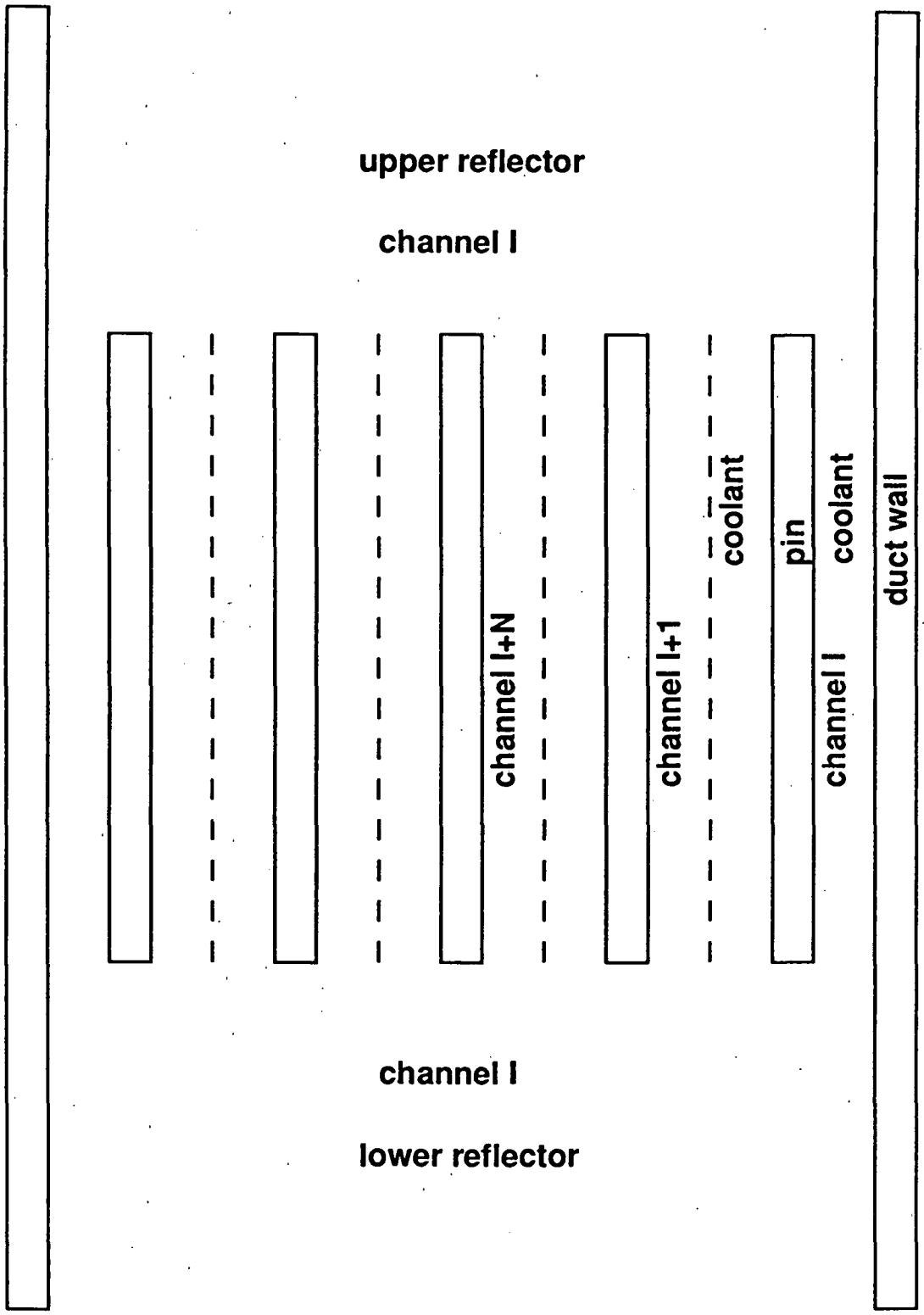

Figure 2. SASSYS-1 Multiple Pin Treatment of a Subassembly

In the new model the coolant in channel I can transfer heat directly to the coolant in channel I-1 and channel I+1. Using correlations of the same form as those used in the THI3D code[6] and the HOTCHAN code[7], the channel-to-channel heat flow per pin per unit height from channel I to channel I+1 is calculated as:

$$Q_{I,I+1} = \left[U_1 \bar{k} + U_2 \bar{C} (w_I + w_{I+1})\right] (T_I - T_{I+1}) \quad (1)$$

where

$\bar{k}$ = average thermal conductivity of the coolant

$\bar{C}$ = average specific heat

w_I = coolant mass flow per pin (kg/s) in channel I,

and

T_I = coolant temperature

In this equation U_1 is a geometry factor for thermal conduction, and U_2 is a product of a turbulent-mixing coefficient and a geometry factor for turbulent mixing between channels. Since a SASSYS-1 channel usually models a group of coolant sub-channels, the values used for U_1 and U_2 must account for a combination of parallel and series heat flow paths between the middle of channel I and the middle of channel i+1. Subassembly-to-subassembly heat transfer is handled in a somewhat simpler manner. For heat transfer from the outer surface of the structure in channel I to the outer surface of the structure in channel J, a constant value is used for the product of the heat transfer coefficient and the heat transfer area per unit height.

2.2 Numerical Methods

Most of the transient heat transfer calculations and flow rate calculations in SASSYS-1 use semi-implicit time differencing in order to obtain stable and accurate solutions

with reasonably long time steps. Before the onset of coolant boiling or pin disruption, time step sizes of a second or more are commonly used; and the code usually runs significantly faster than real time on a Cray XMP computer.

From a numerical computation point of view, the two main tasks in adding the multiple pin model to the code were the coolant-to-coolant heat transfer calculation and the coolant flow rate calculation with parallel flow paths in the pin section. Both of these calculations use semi-implicit time differencing. In the single-pin model, coolant temperatures for all of the radial temperature nodes in the pin, coolant, and structure at one axial node are solved for simultaneously in order to obtain a semi-implicit time differencing solution without iteration. In the new multiple-pin treatment, this concept is carried one step further. At a given axial node, temperatures at all of the radial nodes for all channels representing a subassembly are solved for simultaneously. In the heat transfer calculations, the axial conduction terms, which are small, are treated with explicit forward time differencing so that axial nodes are decoupled and can be treated separately except for the coolant convection terms. The axial coupling due to the coolant convection terms is handled by starting at one end of the subassembly and solving for axial nodes one at a time in the direction of the flow. If flow has reversed in some channels but not in others, the calculation progresses in the direction of the dominant flow; and explicit forward differencing is used for the coolant convection terms in the non-dominant flow direction channels. The subassembly-to-subassembly heat fluxes are calculated with explicit forward differencing in time, and this does impose a stability limit on the time step size. For typical subassembly duct wall thicknesses, the explicit subassembly-to-subassembly heat flux calculation limits the maximum time step size to a value in the range from .25 to .5 seconds. For the coolant flow rate calculations, the incompressible flow momentum equations are linearized about conditions at the beginning of the time step. Then, flows at the end of the step are calculated for all channels in a subassembly simultaneously.

A null transient is used to obtain steady-state temperatures at the start of the regular transient. First all coolant, pin, structure, and reflector temperatures in all subassemblies are set to the coolant inlet temperature. Then, the power levels and coolant flow rates are held

constant while a number of transient heat transfer time steps are made. Since the pin thermal time constant and the coolant transit time through a subassembly are both less than a second, the null transient results converge rapidly if reasonably large time steps are used.

2.3 Detailed Mathematical Treatment

The main computational parts of the new multiple pin model are the heat transfer calculations in the pin section of a subassembly, the coolant flow rate calculations for a subassembly, the subassembly-to-subassembly heat transfer, and changes to the driver routines to call the appropriate new routines at the proper times. The pin section heat transfer calculations are done in two new subroutines: TSHTM3 calculates temperatures in the core and axial blankets, and TSHTM2 calculates temperatures in the gas plenum region. The existing TSHTN1 still calculates temperatures in the reflector zones above and below the pin section, but it was modified. TSHTN1 had to be modified slightly to pick up mixed mean outlet temperatures from the multiple channels representing the pin section. Also, axial conduction in the coolant was added to TSHTN1. The new TSCLM1 routine calculates transient coolant flow rates for a subassembly. The subassembly-to-subassembly heat fluxes are calculated in CHCHFL.

2.3.1 Heat Transfer Calculations in the Core and Axial Blankets: Subroutine TSHTM3

The multiple pin heat transfer calculations for the core and axial blankets in subroutine TSHTM3 are similar to the single pin calculations in the existing subroutine TSHTN3, as described in reference 8. One difference is that TSHTN3 does one time step for one channel each time it is called, whereas TSHTM3 solves for temperatures in all pins or channels representing a subassembly when it is called. Also, TSHTM3 adds extra terms for coolant-to-coolant heat transfer; and TSHTM3 includes axial conduction in the coolant.

Within a fuel pin, one-dimensional radial heat transfer is used. The basic heat transfer equation is:

$$\rho c \frac{\partial T}{\partial t} = \frac{1}{r} \frac{\partial}{\partial r} (kr \frac{\partial T}{\partial r}) + Q \qquad (2)$$

where

T = temperature

ρ = density

c = specific heat

r = radius

k = thermal conductivity

t = time

and

Q = heat source per unit volume.

This part of the calculation in TSHTM3 is identical to the corresponding calculation in TSHTN3.

For the coolant in channel I, the heat transfer calculations are basically one-dimensional in the axial direction, with extra terms for coolant-to-coolant heat transfer from channel I-1 and I+1. The basic heat transfer equation is:

$$\rho c A_c \frac{\partial T}{\partial t} + \frac{\partial}{\partial z} (wcT) = Q_T A_c \qquad (3)$$

where

A_c = coolant flow area

z = axial position

w = coolant mass flow rate

and

Q_T = total heat source per unit volume

The heat source contains a number of terms:

$$Q_T = Q_c + Q_{cc} + Q_{sc} + Q_{ax} + Q'_{I-1,I} - Q'_{I,I+1} \tag{4}$$

where

Q_c = source due to direct heating of the coolant by neutrons and gamma rays,

Q_{cc} = heat flow from cladding to coolant,

Q_{sc} = heat flow from structure to coolant,

Q_{ax} = axial conduction source, given by

$$Q_{ax} = \frac{\partial}{\partial z} k \frac{\partial T}{\partial z} \tag{5}$$

and

$$Q'_{I,I+1} = \frac{Q_{I,I+1}}{A_c} \tag{6}$$

where $Q_{I,I+1}$ is given by equation 1.

Finite differencing in space and time is used to solve these heat transfer equations. Figure 3 shows the axial and radial mesh used for a single channel. In the multiple pin model the pin section mesh is repeated for each channel, but the axial reflector zones are only used in the first channel used to represent a subassembly. At each axial node in the core and axial blankets a number of radial nodes are used for the fuel, three radial nodes are used for the cladding, one node is used in the coolant, and two nodes are used in the structure. All channels representing a subassembly must use the same axial mesh. Also, all subassemblies connected by subassembly-to-subassembly heat transfer must use the same axial mesh.

For a given time step, equations 2 and 3 become linear finite difference equations. The temperatures are known at the beginning of the time step, and the temperatures at the end of the step are the unknowns to be solved for. Semi-implicit time differencing is used for all terms except the axial conduction term Q_{ax}, and the coolant-to-coolant terms $Q_{I-1,I}$ and $Q_{I,I+1}$. The

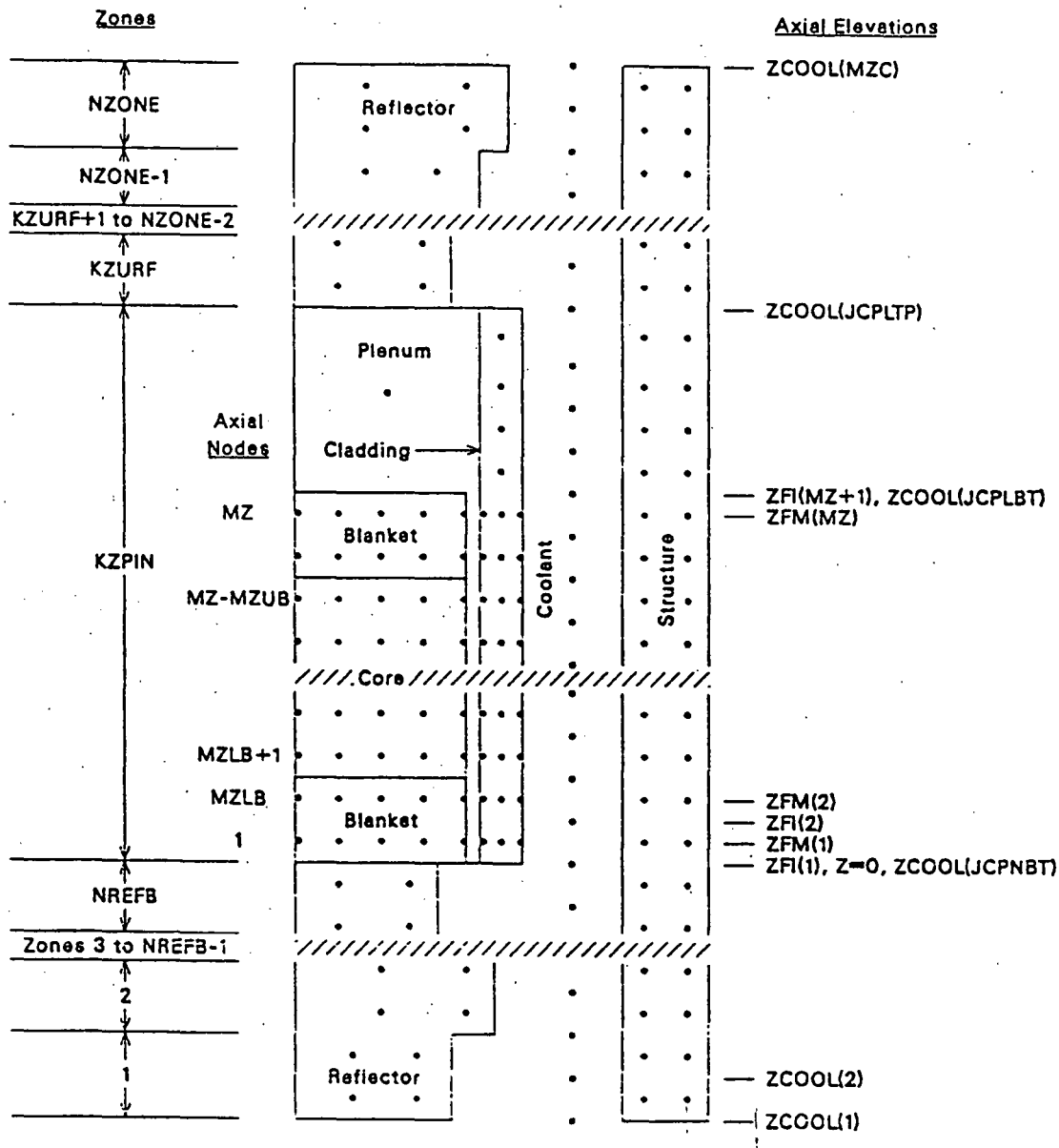

Figure 3. Schematic of SASSYS Channel Discretization

$Q_{I,I+1}$ axial conduction term is calculated explicitly based on temperatures at the beginning of the time step. The coolant-to-coolant terms are calculated fully implicitly, using the coolant flow rates and temperatures at the end of the step.

After finite differencing for one axial node, one obtains N simultaneous linear equations in N unknowns, where the unknowns are the temperatures at the end of the time step for all radial nodes in all channels representing the subassembly. These equations are solved by Gaussian elimination. The equations are basically tri-diagonal, with extra non-tri-diagonal terms for coolant-to-coolant heat transfer between channels. No full N by N matrix is ever set up by TSHTM3, and a general full matrix solution package is not used. Instead, only non-zero terms are computed and stored; and the Gaussian elimination solution was written specifically for this set of equations. The result is that the storage requirements vary linearly, rather than quadratically, with the maximum allowable value for N; and the computation time varies linearly, rather than quadratically,with the actual value of N.

2.3.2 Heat Transfer Calculations in the Gas Plenum Region: Subroutine TSHTM2

Subroutine TSHTM2 does the heat transfer calculations for one time step for all axial nodes in the gas plenum region for all channels representing a subassembly when it is called. TSHTM2 is similar to TSHTM3, but TSHTM2 deals with fewer radial nodes. As shown in Figure 4, in the plenum region there are still two radial nodes in the structure and one in the coolant; but there is only one in the cladding; and there are no fuel nodes. Instead of fuel temperatures there is one gas temperature common to all of the axial nodes is a pin. As in TSHTM3, for a given axial node TSHTM2 solves simultaneously for temperatures at all radial nodes in all channels representing a subassembly.

One special problem in TSHTM2 is the gas temperature, which is common to all axial nodes in the gas plenum region of a pin. Axial nodes are handled one at a time, rather than simultaneously, whereas a semi-implicit time differencing treatment would require solving for

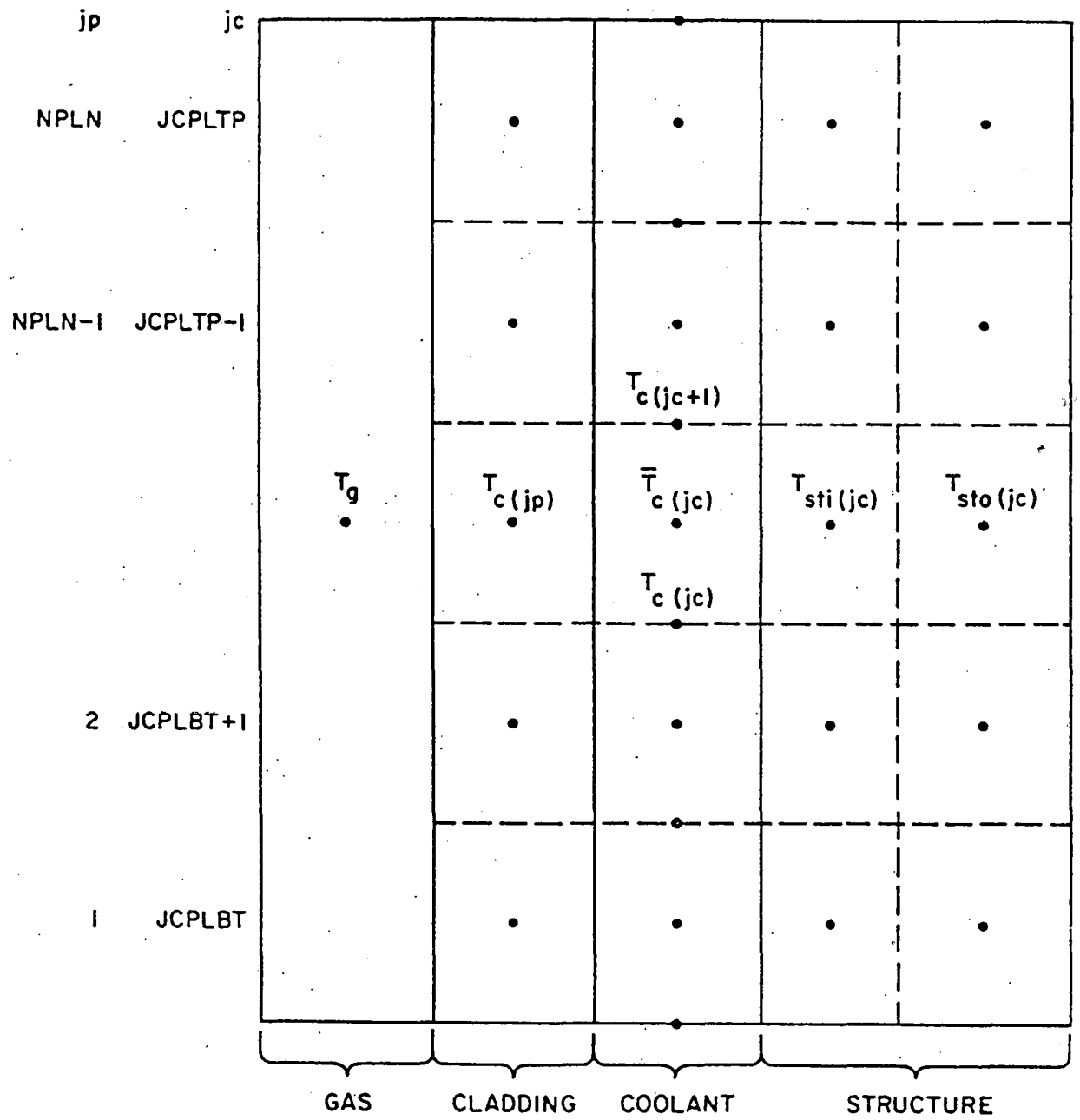

Figure 4. Radial Temperature Nodes, Gas Plenum Region

all axial nodes simultaneously. The new multiple-pin TSHTM2 routine handles this problem in a simpler manner than the old single-pin TSHTN2. The way that the gas temperature is handled in TSHTM2 is to calculate a separate gas temperature for each axial node. At the beginning of the time step, the gas temperatures at all axial nodes are set to one common value. Then separate values are calculated for each axial node at the end of the step. Finally, an average of the separate values is calculated for the one common value at the end of the step.

2.3.3 Coolant Flow Rates: Subassembly TSCLM1

The coolant flow rate calculation for a subassembly in the multiple-pin routine TSCLM1 is much more complex than the corresponding calculation in the single pin routine TSCNV1. As shown in Figure 2, the multiple pin calculation involves multiple parallel flow paths in the pin section, in series with single flow paths in the reflector regions. Therefore, the multiple-pin routine TSCLM1 was written from scratch, rather than starting from the single pin TSCNV1 routine.

Figure 5 illustrates the main variables used in TSCLM1. Incompressible flow is used for these calculations, so conservation of mass gives

$$N_I \, w_r = \sum_k w_{pk} \, N_k \tag{7}$$

where

w_r = coolant mass flow rate per pin in the reflector zones,

w_{pk} = pin section coolant mass flow rate per pin in channel k,

N_k = number of pins in channel k,

and

I = channel number of the first channel representing the subassembly.

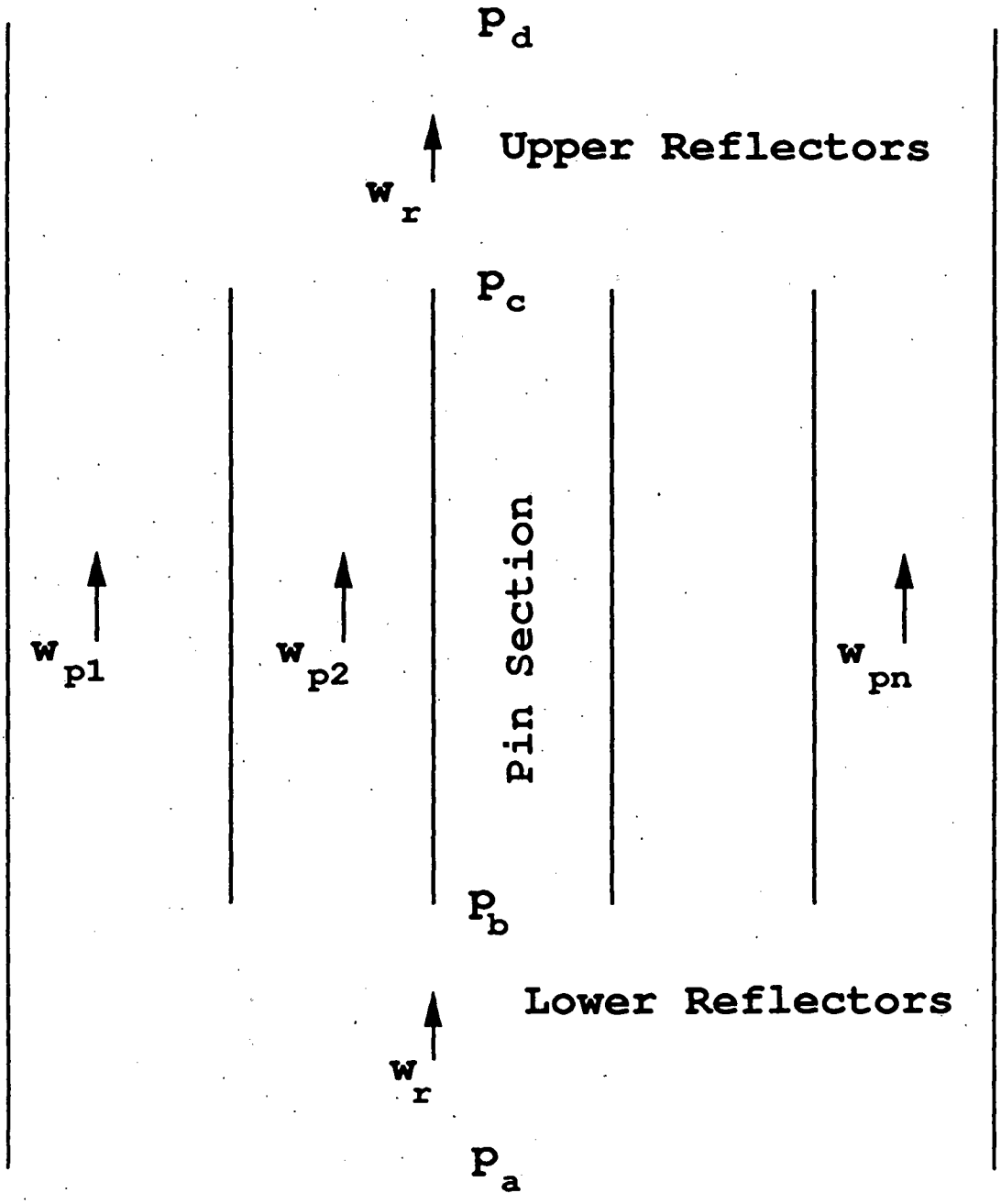

Figure 5. Subassembly Coolant Flows

The momentum equation for the pin section is

$$\frac{L_p}{A_{cpk}} \frac{dw_{pk}}{dt} = p_b - p_c - \Delta p_{pk} \tag{8}$$

where

L_p = length of the pins,

A_{cpk} = coolant flow area in channel k in the pin section,

t = time,

p_b = coolant pressure at the bottom of the pins,

p_c = coolant pressure at the top of the pins,

$$\Delta p_{pk} = \text{pressure loss} = \sum_{jc=JCPNBT}^{JCPNTM} \Delta p_{kjc} \tag{a}$$

jc = axial coolant node,

JCPNBT = first axial node in the pin section

JCPNTM = last axial node in the pin section,

and

Δp_{kjc} = pressure loss in axial node jc of channel k.

The pressure loss contains a number of terms:

$$\Delta p_{kjc} = \Delta p_{frkjc} + \Delta p_{grkjc} + \Delta p_{orfkjc} + \Delta p_{acckjc} \tag{10}$$

where

$$\Delta p_{frkjc} = \text{friction loss} = \frac{f_{kjc} \Delta z_{jc} w_{pk} | w_{pk} |}{2 \bar{\rho}_{ckjc} A_{cpk} D_{hpk}} \tag{11}$$

$$\Delta p_{grpjc} = \text{gravity head} = g \bar{\rho}_{ckjc} \Delta z_{jc} \tag{12}$$

$$\Delta p_{orf\,kjc} = \text{orifice loss} = \frac{K_{orkjc}\, w_{pk} \mid w_{pk} \mid}{2\bar{\rho}_{ckjc} A_{cpk}^2} \tag{13}$$

$$\Delta p_{acckjc} = \text{acceleration term} = \frac{w_{pk}^2}{A_{cpk}^2}\left[\frac{1}{\rho_{ckjc+1}} - \frac{1}{\rho_{ckjc}}\right] \tag{14}$$

Δz_{jc} = axial node length,

f_{kjc} = friction factor in channel k at node jc,

ρ_{ckjc} = coolant density at bottom of node jc in channel k,

$\bar{\rho}_{ckjc}$ = average coolant density in node jc in channel k,

D_{hpk} = hydraulic diameter,

and

K_{orkjc} = orifice coefficient in node jc of channel k.

The friction factor is calculated as

$$f_{kjc} = \begin{cases} A_{fr}\, R_e^{b_{fr}} & \text{if } R_e \geq R_{eL} \\ A_{fL}/R_e & \text{if } R_e < R_{eL} \end{cases} \tag{15}$$

where

A_{fr}, b_{fr} = correlation coefficients for the turbulent range,

$$R_e = \text{Reynolds number} = \frac{D_{hpk} \mid w_{pk} \mid}{\mu_{kjc} A_{cpk}} \tag{16}$$

μ_{kjc} = viscosity of the coolant.

R_{eL} = Reynolds number for transition from turbulent to laminar flow,

and

A_{fL} = laminar friction factor correlation coefficient.

After semi-implicit finite differencing in time and linearization of the pressure drop terms, applying equation 8 to a time step from t to t + Δt gives

$$\frac{L_p}{A_{cpk}} \frac{\Delta w_{pk}}{\Delta t} = p_b(t) + \theta_2 \Delta p_b - p_c(t) - \theta_2 \Delta p_c - \Delta p_{pk}(t) - \theta_2 \Delta w_{pk} K_{wpk} \tag{17}$$

where

$$\Delta w_{pk} = w_{pk}(t+\Delta t) - w_{pk}(t) \tag{18}$$

$$\Delta p_b = p_b(t+\Delta t) - p_b(t) \tag{19}$$

$$\Delta p_c = p_c(t+\Delta t) - p_c(t) \tag{20}$$

θ_2 = degree of implicitness

$$\theta_1 = 1 - \theta_2 \tag{21}$$

$$K_{wpk} = \sum_{jc=JCPNBT}^{JCPNTM} K_{wpkjc} \tag{22}$$

$$K_{wpkjc} = \frac{\partial p_{kjc}}{\partial w_{pk}} = K_{frkjc} + K_{workjc} + K_{acckjc} \tag{23}$$

$$K_{frkjc} = \begin{cases} (2+b_{fr}) \dfrac{\Delta p_{frkjc}(t)}{w_{pk}(t)} & \text{if } R_{ekjc} \geq R_{et} \\ \dfrac{\Delta p_{frkjc}(t)}{w_{pk}(t)} & \text{if } R_{ekjc} < R_{et} \end{cases} \tag{24}$$

$$K_{workjc} = \frac{2\Delta p_{orfkjc}(t)}{w_{pk}(t)} \tag{25}$$

and

$$K_{acckjc} = \frac{2\Delta p_{acckjc}(t)}{w_{pk}(t)} \tag{26}$$

Equation 17 can then be written as

$$\Delta p_b - \Delta p_c = d_{0pk} + d_{1pk}\,\Delta w_{pk} \tag{27}$$

where

$$d_{0pk} = \frac{p_c(t) - p_b(t) + \Delta p_{pk}(t)}{\theta_2} \tag{28}$$

and

$$d_{1pk} = \frac{L_p/A_{cpk} + \theta_2 \Delta t\, K_{wpk}}{\theta_2\, \Delta t} \tag{29}$$

Applying a similar process to the upper and lower reflector regions gives:

$$\Delta p_b = D_{0\ell} + D_{1\ell} \sum_k \Delta w_{pk} \tag{30}$$

and

$$\Delta p_c = D_{0u} + D_{1u} \sum_k \Delta w_{pk} \tag{31}$$

where

$$D_{0\ell} = \frac{\theta_1\, p_a(t) + \theta_2 p_a\,(t+\Delta t) - p_b\,(t) - \Delta p_\ell(t)}{\theta_2} \tag{32}$$

$$D_{1\ell} = \frac{-\sum_{KZ=1}^{KZPIN-1} L_{KZ}/A_{cKZ} - \theta_2 \Delta t \, K_{w\ell}}{\theta_2 \Delta t} \tag{33}$$

$$D_{0u} = \frac{\theta_1 p_d(t) + \theta_2 \, p_d(t+\Delta t) - p_c(t) + \Delta p_u(t)}{\theta_2} \tag{34}$$

$$D_{1u} = \frac{\sum_{KZ=KZPIN+1}^{KZM} L_{KZ}/A_{cKZ} + \theta_2 \Delta t \, K_{wu}}{\theta_2 \Delta t} \tag{35}$$

L_{KZ} = length of zone kz

A_{cKZ} = coolant flow area in zone kz

KZPIN = axial zone number of the pin section

KZM = last zone number

$$\Delta p_\ell = \sum_{jc=1}^{JCPNBT-1} \Delta p_{rjc} \tag{36}$$

$$\Delta p_u = \sum_{jc=JCPNTP}^{MZCM1} \Delta p_{rjc} \tag{37}$$

Δp_{rjc} = pressure loss in node jc of a reflector zone

JCPNBT = first axial node in pin section

JCPNTP = first axial node above the pin section

MZCM1 = last axial node

$$K_{w\ell} = \frac{\partial \Delta p_\ell}{\partial w_r} \tag{38}$$

and

$$K_{wu} = \frac{\partial \Delta p_u}{\partial w_u} \tag{39}$$

Then, combining Eqs. (27) and (30) gives

$$\Delta p_b = B_0 + B_1 \, \Delta p_c \tag{40}$$

where

$$B_o = \frac{D_{o\ell} - D_{1\ell} \, S_1}{1 - D_{1\ell} \, S_o} , \tag{41}$$

$$B_1 = \frac{-D_{1\ell} S_o}{1 - D_{1\ell} S_o} , \tag{42}$$

$$S_o = \sum_k \frac{1}{d_{1pk}} , \tag{43}$$

and

$$S_1 = \sum_k \frac{d_{opk}}{d_{1pk}} , \tag{44}$$

Similarly, combining Eqs. (27) and (31) gives

$$\Delta p_c = C_o + C_1 \, \Delta p_b \tag{45}$$

where

$$C_o = \frac{D_{ou} - D_{lu} S_l}{1 + D_{lu} S_o} , \tag{46}$$

and

$$C_l = \frac{D_{lu} S_o}{1 + D_{lu} S_o} . \tag{47}$$

Combining Eqs. (40) and (45) gives

$$\Delta p_c = \frac{C_o + C_l B_o}{1 - C_l B_l} \tag{48}$$

Then Δp_b can be obtained from Eq. (40) and Δw_{pk} can be obtained from Eq. (27) for each channel.

After p_b, p_c, and the coolant flow rates have been calculated for the end of the time step, it is possible to calculate the pressures. The pressure is calculated at the axial node boundaries. p_{pkjc} is the pressure at the bottom (inlet end) of node jc in channel k. First, the nodal pressure loss at $t+\Delta t$ is calculated as

$$\Delta p_{pkjc}(t+\Delta t) = \Delta p_{kjc}(t) + K_{wpkjc} \Delta w_{pk} \tag{49}$$

and Δp_{pk} $(t+\Delta t)$ is calculated from Eq. (9). Then Eq. (8) is used to obtain $\frac{dw_{pk}(t+\Delta t)}{dt}$.

Integrating the momentum equation over one axial node gives

$$\frac{\Delta z_j}{A_{cpk}}\frac{dw_{pk}}{dt} = p_{pkjc} - p_{pkjc+1} - \Delta p_{kjc} \tag{50}$$

Starting by setting

$$p_{pkJCPNTP} = P_c \tag{51}$$

the code marches down the channel, using Eq. (50) to obtain p_{pkjc} after p_{pkjc+1} has been calculated. A similar procedure is used for calculating the pressures in the upper and lower reflector zones.

The equation used to compute the degree of implicitness as a function of time step size in TSCMV1 is

$$\theta_2 = \frac{a + bx + x^2}{2a + cx + x^2} \tag{52}$$

where

$$\begin{aligned} x &= \Delta t/\tau \\ \tau &= \text{a time constant} \\ a &= 6.12992 \\ b &= 2.66054 \end{aligned} \tag{53}$$

and

$$c = 3.56284$$

The basis for this expression is given in Appendix 2.1 of reference 8. For a single channel treatment, the time constant, τ would be

$$\tau = \frac{\sum_{KZ=1}^{KZM} \frac{L_{KZ}}{A_{cKZ}} + \left(\frac{L_i}{A}\right)_i + \left(\frac{L_i}{A}\right)_x}{K_{wpk} + K_{wl} + K_{wu}} \tag{54}$$

where

$\left(\frac{L_i}{A}\right)_i$ = extra coolant inertia term at the subassembly inlet to account for inertia of the coolant in the inlet plenum,

and

$\left(\frac{L_i}{A}\right)_x$ = same for the subassembly outlet.

Since a simultaneous solution of flows in all channels of an assembly plus the lower and upper reflector zones is required, the overall time constant is calculated as

$$\tau = \frac{\frac{L_p}{\sum_k A_{cpk}} + \sum_{kx \neq KZPIN} \frac{L_{KZ}}{A_{cKZ}} + \left(\frac{L_i}{A}\right)_i + \left(\frac{L_i}{A}\right)_x}{K_{wl}+K_{wu} + \frac{1}{\sum_k \frac{1}{k_{wpk}}}} \tag{55}$$

2.3.4 Subassembly-to-Subassembly Heat Fluxes: Subroutine CHCHFL

SASSYS-1 contained an old subassembly-to-subassembly heat transfer capability which was never used, except for a few test calculations. This old capability had the advantage that it was numerically stable for any time step size, but it had the disadvantage that it did not conserve energy except in the limit of small time step sizes. Therefore, a new subassembly-to-subassembly heat transfer capability has replaced the old one. The new capability conserves energy, but it imposes a stability limit on the maximum time step size. The stability limit is typically in the range of .2-.5 seconds.

At the beginning of each main time step, subroutine CHCHFL is called to calculate the heat flow per pin per unit length from the outer structure node of channel I to the outer structure node of channel J as

$$Q_{chIJ,jc} = \frac{(HA)_{IJ}}{N_{PJ}\, N_{SJ}} (T_{SOI,jc} - T_{SOJ,jc}) \tag{56}$$

where

$T_{SOI,jc}$ = outer structure node temperature in channel I at axial node jc,

N_{pJ} = number of pins per channel in channel J,

N_{sJ} = number of subassemblies represented by channel J,

and

$(HA)_{IJ}$ = user supplied product of the heat transfer coefficient and the total contact perimeter between channel I and Channel J.

The heat flows are calculated for all axial nodes, but only for I, J pairs specified by the user.

The values of the heat flows are calculated using temperatures at the beginning of the main time step, but they are used for the whole step. The heat flow values are multiplied by heat transfer time step sizes to obtain heat source terms for the outer structure node temperature calculations.

2.3.5 Data Management for the Multiple Pin Option

Implementation of the multiple pin option required modification of the data management philosophy is SASSYS-1. Basically, the data management in SASSYS-1 was based on the idea of treating one channel at a time, and data for only one channel was accessible at any given time. With the multiple pin treatment, it is necessary to deal with a number of channels simultaneously; so the old data management scheme was not sufficient.

The data management scheme is SASSYS-1 goes back many years to the SAS3D code. It was designed for optimum performance and portability on an earlier generation of computers with limited memory, sometimes a two level memory structure, and an ANSI Standard FORTRAN 66 that severely limited the form of expressions that could be used for array subscripts. With current computers, these considerations no longer apply. Memory is plentiful, explicit two level memory structures are not used, and the current ANSI Standard FORTRAN 77 allows much more general subscript expressions. Therefore, it was possible to come up with modifications to the SASSYS-1 data management scheme that make it possible to access data for a number of channels simultaneously without impairing performance or portability.

The SAS3D data management scheme was developed in response to problems with the earlier SAS3A code. SAS3A handled channel-dependent data by adding a channel subscript to all channel-dependent variables. The channel subscript was dimensioned for 10 channels. All data, other than a few temporary variables, was stored in COMMON blocks that were available to all subroutines. This scheme had the advantage that all data for all channels was always available. This scheme also had some disadvantages, both obvious and subtle. One disadvantage was that the code required 10 channels worth of memory any time it was run, even if only one channel was actually being used for a particular case. At the time the SAS3A code was in use, most computers did not have enough memory to fit 10 channels worth of data. Even if enough memory was available, using a large amount of memory often required the use of non-standard, system-dependent features that reduced code portability and made it difficult to take the code that ran on one computer and get it to run on another computer. Another obvious disadvantage was that SAS3D could not run any case bigger than 10 channels, even if enough memory was available. A subtle disadvantage of the use of a channel subscript on arrays is that many computers use a data cache between the central processor and main memory. With a dimension of 10 for the channel subscript, about 90% of the data in the cache at any time may be for channels that are not currently being computed. Thus, the effectiveness of the cache is greatly reduced, and the code runs slower. One common way some of these problems are handled is through the use of the standard FORTRAN variable dimensioning capability that allows setting of maximum dimensions at run time, based on the size of the problem being run. The standard variable dimensioning approach is impractical or impossible with the

SAS3A/SAS3D/SASSYS-1 codes because they use literally thousands of separate variable names for channel-dependent quantities.

The data management scheme developed for SAS3D and still used in SASSYS-1 uses a working memory and a storage area. All calculations are done with the data in the working memory. Data is stored in the storage area when it is currently not needed. The working memory contains both temporary variables and permanent variables. All permanent variables and most temporary variables are put in COMMON blocks. The permanent variables are saved in the storage area when they are not needed in the working memory, whereas temporary variables are not saved from time step to time step. Data is moved from the working memory to the storage area and back in large blocks called data packs. Each data pack contains variables for only one channel or maybe for one module for one channel. The working memory is always a part of the central memory, whereas the storage area could in principle be either a dynamically allocated section of main memory or it could be on a disk. With a two level memory architecture, the working memory is in the smaller but faster level, whereas the storage area can be put in the larger but slower level. Data packs are moved between working memory and the storage area by a single subroutine, called DATMOV, which can be optimized for a particular computer. Code portability issues are then limited to the one routine DATMOV.

The modifications to the data management scheme in SASSYS-1 for the multiple pin option are based on the fact that currently the storage area is always in a dynamically allocated section of main memory. Explicit two level memory architectures are not currently used; and putting the storage area on a disk has proved to be impractical, because disk I/O is much too slow to keep up with the central processor speeds for SASSYS-1. Also, memory is now cheap, and plenty of memory is available on all machines where SASSYS-1 is likely to be run. Another aspect of the data management that is taken advantage of in the modifications is that the ordering of variables for a channel in the data storage area is the same as the ordering in the working area of blank common. When more than one channel is used to represent a subassembly, the data packs for the first channel are still moved into the working area by DATMOV, but the data for the rest of the channels stays in the storage area where it is accessed directly by adding the appropriate pointers to array subscripts. Thus, if T2(I,J) is a temperature

at radial node I of axial node J, then a multiple-pin routine such as TSHTM3 refers to this variable as T2(I+IPT,J), where IPT is the channel-dependent pointer. For the first channel in the subassembly, IPT is set to 0, since DATMOV has put the data for the first channel into the COMMON block where the FORTRAN compiler expects it to be. For other channels, IPT is set to the offset between the working memory location and the storage area location for the channel. Since data packs are put into blank COMMON in the working memory in the same order that they are stored in the storage area, the value of the pointer for all floating point variables for a given channel is the same. Also, the pointer for all integers in a channel is the same. The pointer for a floating pint variable will be different from the pointer for an integer if the word length of integers is different from the word length of floating point variables. The channel dependent pointers are computed once at the beginning of the run and stored in a labeled COMMON block where they can be used by all routines. The subassembly-to-subassembly heat flux routine CHCHFL accesses temperatures from many different channels. CHCHFL uses only pointers to access different channels. It does not use DATMOV at all.

3.0 EXPERIMENTAL VERIFICATION

A series of thermal-hydraulics tests[9] has been performed in EBR-II (Experimental Breeder Reactor-II) to demonstrate that a properly designed LMR with metal fuel can survive a number of anticipated transients without scram[10]. One of these tests[11], the SHRT-45 (Shut-down Heat Removal Test-45) was a loss-of-primary-flow-without-scram from full power and full flow. This test was picked to use for verification of the new multiple pin model for a number of reasons. First, this is the type of transient that SASSYS-1 was designed for and is often used for. Second, detailed temperature data is available for this test from thermocouples in the coolant in the XX09 instrumented subassembly. Third, this was the most severe of the loss-of-flow-without-scram tests run in EBR-II.

3.1 SHRT-45 Test Description and Calculational Model

The SASSYS-1 model for this test included a multi-channel core description with emphasis on the details of the XX09 instrumented subassembly, a detailed thermal hydraulic model for the primary coolant system, a detailed thermal hydraulic model for the intermediate heat transport system, and a simple steam generator model. Nothing beyond the steam generators was modeled, and even the steam generators had very little influence on the core during the time scale of interest in this test. On the other hand, the primary coolant system behavior was important in this test; and one important aspect was the behavior of the two primary loop centrifugal pumps which drove the coolant through the core in the earlier part of the transient. In the later part of the transient the pumps had stopped, and primary loop natural circulation heads were dominant. The centrifugal pump model used in these calculations was the homologous pump model described in reference 12, based on the work of Wylie and Streeter[13,14].

The whole core was represented in the calculational model. Table 1 describes the 34 channels used for this case. Eight channels were used for single pin treatments of the bulk of the driver subassemblies, the control rod channels, the stainless steel reflector subassemblies, and some low power irradiation experimental subassemblies that were in the core. In addition, two channels were used for single pin representations of XX09 and another instrumented subassembly, XX10. Some of the subassemblies neighboring XX09 were similar enough in power and flow to be lumped together, so eight channels (channels 11-18) were used for two-pin representations of each of four neighboring subassemblies. For each of the neighboring subassemblies, one channel was used to represent the outer coolant and pins near XX09, and the other channel was used for the rest of the subassembly. Six channels were used for a multiple pin representation of XX09. Channels 25-30 were used for two-pin representations of the subassemblies next to XX10, and channels 31-34 were used for XX10. XX10 results are not included in this report. The steady-state channel powers and flows used in this model are based on the subassembly values given in reference 15.

Table 1. SASSYS-1 Channel Description for SHRT-45 Analysis

Channel	Number of Subassemblies	Number of Pins per Subassembly	Power per Pin (kW)	Coolant Flow Rate per Pin (kg/sec.)	Power/flow	Description
1	0	1	6.280	.04178	150.31	XX09 average pin
2	0	1	.9168	.01951	46.99	XX10 average pin
3	10	61	7.118	.05862	121.43	control, safety rods
4	21	1	16.27	.16832	96.67	reflectors, rows 7,8
5	7	91	.1997	.00761	26.24	low power experiments
6	8	91	3.598	.04082	88.14	P, rows 1,2,3
7	19	91	7.286	.05806	125.49	drivers, rows 3,4
8	8	91	6.499	.04723	137.60	drivers, row 5
9	36	91	6.081	.04032	150.82	22 HFD, row 6; 14D, row 7
10	4	91	2.982	.02790	106.88	P, rows 6,7
11	1	11	.259	.00801	32.33	X320 (4D2), pins near XX09
12	1	80	.259	.00706	36.69	remainder of X320
13	1	14	7.497	.10805	69.39	driver (4D3), outer row
14	1	77	7.497	.04489	167.01	remainder of (4D3)
15	2	14	6.77	.09329	72.57	drivers (5D2, 5D4), outer row
16	2	77	6.77	.03876	174.66	remainder of (5D2, 5D4)
17	2	14	6.88	.08251	83.38	HFD (6D3, 6D4), outer row
18	2	77	6.88	.03428	200.70	remainder of (6D3,6D4)
19	1	1	3.8	.467	8.14	XX09, thimble flow region
20	1	13	6.218	.07419	83.81	XX09, outer coolant row
21	1	21	6.218	.03313	187.68	XX09, next coolant row
22	1	15	6.218	.03313	187.68	XX09, next coolant row
23	1	9	6.218	.03313	187.68	XX09, next coolant row
24	1	3	6.218	.03123	199.07	XX09 center
25	1	14	6.513	.10809	60.26	X400 (4C1), outer row
26	1	77	6.511	.04491	144.98	remainder of X400
27	4	14	6.497	.08793	73.89	2 D (5B4,5C2), 2 HFD (6B5, 6C2)
28	4	77	6.497	.03653	177.85	remainder of 2 D, 2 HFD
29	1	14	3.062	.05511	55.56	P (6C1), outer row
30	1	77	3.062	.02289	133.77	remainder of (6C1)
31	1	1	.35	.0643	5.44	XX10 thimble flow region

Channel	Number of Subassemblies	Number of Pins per Subassembly	Power per Pin (kW)	Coolant Flow Rate per Pin (kg/sec.)	Power/flow	Description
32	1	7	.898	.0245	36.65	XX10 outer coolant row
33	1	9	.898	.01123	79.96	XX10 next coolant row
34	1	3	.898	.01123	79.96	XX10 inner coolant row

Note: P = 1/2 driver fuel, 1/2 SST

D = MK2 driver

HFD = high flow driver

Numbers in parenthesis indicate core location: (4D3) indicates row 4, sector D, location 3 numbered clockwise in the sector.

The XX09 instrumented subassembly[16] is a 61 element subassembly containing 59 Mark II fuel elements and two conduit tubes. The conduits provide a passage through the core for thermocouple leads. Twenty-two of the fuel elements have their standard spacer wires replaced by spacer wire thermocouples, providing temperature measurements at various elevations. XX09 simulates a driver subassembly. It is almost identical to a Mark II driver subassembly, except in XX09 the outer row of fuel pins is replaced by an extra hex can wall and a thimble flow region.

Figure 1 shows the SASSYS-1 channel model used to treat XX09 for these calculations. This figure also shows the locations of a row of spacer wire thermocouples running from corner to corner at the top of the core and another row of thermocouples located 14 cm. above the top of the core. The readings from these thermocouples were used for comparison with calculated temperatures. The SASSYS-1 channels model concentric rows of coolant channels, and the thermocouples are located in the centers of these rows except for the 14TC thermocouple on pin 39.

Outside of the subassembly wall there is a thimble flow region separating the subassembly wall from an outer thimble wall. This region is filled with coolant, and there is a small flow rate through the region. A separate SASSYS-1 channel (channel 19) is used to model the thimble flow region. This region required special modeling in SASSYS-1. There are no fuel pins in the thimble flow region, but SASSYS-1 puts a pin in each channel. Therefore, the pin in channel 19 was made very small, with negligible heat capacity and no power. The heat flow from the outside of the subassembly wall to the thimble flow region was a special problem. The structure in channel 20 models the subassembly wall, so the multiple pin model was modified to allow for heat transfer directly from the outer structure node of one channel (channel 20) to the coolant of another channel (channel 19). The structure of channel 19 represents the thimble wall. Subassembly-to-subassembly heat flow was modeled from this wall to the neighboring subassemblies.

The nominal size of the hex can is slightly larger than the size needed to accommodate the pin bundle with a pitch determined by the nominal values for the pin diameter and the spacer wire, leaving a slight amount of extra room in the subassembly. For these calculations, it was assumed that the center 7 pins were spaced as tight as the spacer wire would allow, and the extra space was distributed evenly over the rest of the subassembly. Therefore, channel 24, representing the center of the subassembly, has a slightly smaller coolant flow area per pin and a slightly lower initial flow rate than channels 21-23. Channel 20 has a larger coolant flow area and flow rate because of the extra space at the edge of the pin bundle.

Since the purpose of these calculations was verify the multiple pin thermal hydraulic model, reactivity feedback was not calculated. Instead, the power level was specified as a function of time during the transient, using the measured fission power and a computed decay heat power. The decay heat was calculated from the ANSI light water reactor standard[16] using the irradiation history for the core loading.

Two special problems in the modelling of XX09 were obtaining the correct pressure drop vs. coolant flow rate characteristics for the subassembly and obtaining the coolant-to-coolant heat transfer parameters U_1 and U_2 of Equation 1.

3.1.1 Hydraulic Modelling of XX09

The pressure drop vs. flow rate characteristics of XX09 were measured in water flow tests before the subassembly was put into the reactor. When the usual SASSYS-1 model was set up for this subassembly with the orifice pressure drop adjusted to give the measured total pressure drop at nominal flow, it was found that the calculated pressure drop at lower flows agreed poorly with the measured values. Since most of the pressure drop in XX09 is through the inlet orifice holes, the treatment of the orifice pressure drop must be the main cause of the discrepancy. SASSYS-1 assumes that the pressure drop through an orifice is proportional to the square of the flow, with an orifice coefficient that is independent of Reynolds number. The XX09 measurements indicate that the orifice coefficient is a function of Reynolds number; and the pressure drop through the orifice holes is proportional to the flow raised to the Nth power, where N is less than 2. Therefore, the hydraulic modelling of XX09 was adjusted to match the measured behavior by adding fictitious friction pressure drop to the flow meter region and subtracting a corresponding amount from the orifice. A similar treatment was used for the Mark II driver subassemblies.

To obtain the turbulent friction factor for XX09, the pin bundle multiplier of Novendstern[18] was used with the smooth tube friction factor of Moody[19]. The resulting friction factor was evaluated at a number of values of the Reynolds number and these results were fit in the form used by SASSYS-1. The laminar friction factor for the pin bundle was obtained from the correlation of Engel, Markley, and Bishop[20]. The correlation used for XX09 and for the Mark II drivers was

$$f = \begin{cases} .3744\ Re^{-.258} & \text{if } Re \geq 2410 \\ 121/Re & \text{if } Re < 2410 \end{cases} \qquad (57)$$

where

f = friction factor

and

Re = Reynolds number.

The transition at Re = 2410 gives a continuous function with no jump in f.

The pressure drop vs. flow characteristics of XX09 were measured by Wendte[21,22] in water tests over the range from nominal flow down to very low flow rates and even into reverse flow. After conversion to sodium at 800°F. (699.8K), the normal flow direction measurements can be fit by

$$\Delta p(\text{Pa}) = \begin{cases} 2.668 \times 10^5 \left[\frac{w}{w_o}\right]^{1.88} & \text{if } \frac{w}{w_o} \geq .1 \\ 1.725 \times 10^5 \left[\frac{w}{w_o}\right]^{1.69} & \text{if } .1 > \frac{w}{w_o} \geq .02 \\ 5.847 \times 10^4 \left[\frac{w}{w_o}\right]^{1.413} & \text{if } .02 > \frac{w}{w_o} \geq .0053 \\ 6719 \frac{w}{w_o} & \text{if } .0053 > \frac{w}{w_o} \geq 0 . \end{cases} \tag{58}$$

where

Δp = pressure drop, other than gravity lead

w = coolant flow rate

w_o = nominal flow rate = .04364 kg/s = 49.7 gpm

At higher flow rates ($w/w_o > .1$) this expression fits all of the data points to within a few percent, but at lower flow rates there is more scatter in the data. At the low end ($w/w_o < .005$) there is a scatter of about 20% in the data.

Figures 6 and 7 show the correlations of equation 58 for XX09 pressure drop vs. flow with 800°F sodium. Also shown on these figures are the results SASSYS-1 would give with nominal dimensions used to calculate the friction and with a flow-squared orifice pressure drop. For the SASSYS-1 results, the orifice coefficient is set to the value required to match the measured total pressure drop at nominal flow. The results calculated with a flow-squared orifice drop deviate significantly from the measured values. At 5-7% of nominal flow, which is the flow range in SHRT-45 after the first 100 seconds, the deviation is about 15%. This deviation is much larger than the scatter in the measurements in this range.

At nominal flow, friction accounts for about 25% of the total pressure drop, and the orifice accounts for the rest. If the friction pressure drop is proportional to the flow raised to the 1.742 power, then the orifice pressure drop would have to be proportional to the flow raised to the 1.925 power in order to give the measured result that the total pressure drop is proportional to the flow raised to the 1.88 power at higher flow rates. In order to provide better agreement between the calculated and measured pressure drop behavior of XX09, the hydraulic diameter in the flow meter section below the core was reduced from its actual value of .015875 meters (5/8") to .008 m. for the SASSYS-1 calculations. This increased friction loss, and the orifice coefficient was reduced by a corresponding amount. The results after these adjustments are also shown in Figures 6 and 7. With these adjustments, the calculated and measured values agree well over the whole range of flows. For the Mark II drivers, similar adjustments were made: 25% of the orifice pressure drop was converted to friction.

3.1.2 Coolant-to-Coolant Heat Transfer Coefficients

For the thermal conduction part of the coolant-to-coolant heat transfer coefficients, an empirical shape factor correlation by Fukuda[23] was used to obtain the shape factors for heat transfer between adjacent coolant subchannels. The correlation is:

$$U_1 = 1.38\ (S/D)^{-674} \qquad (2)$$

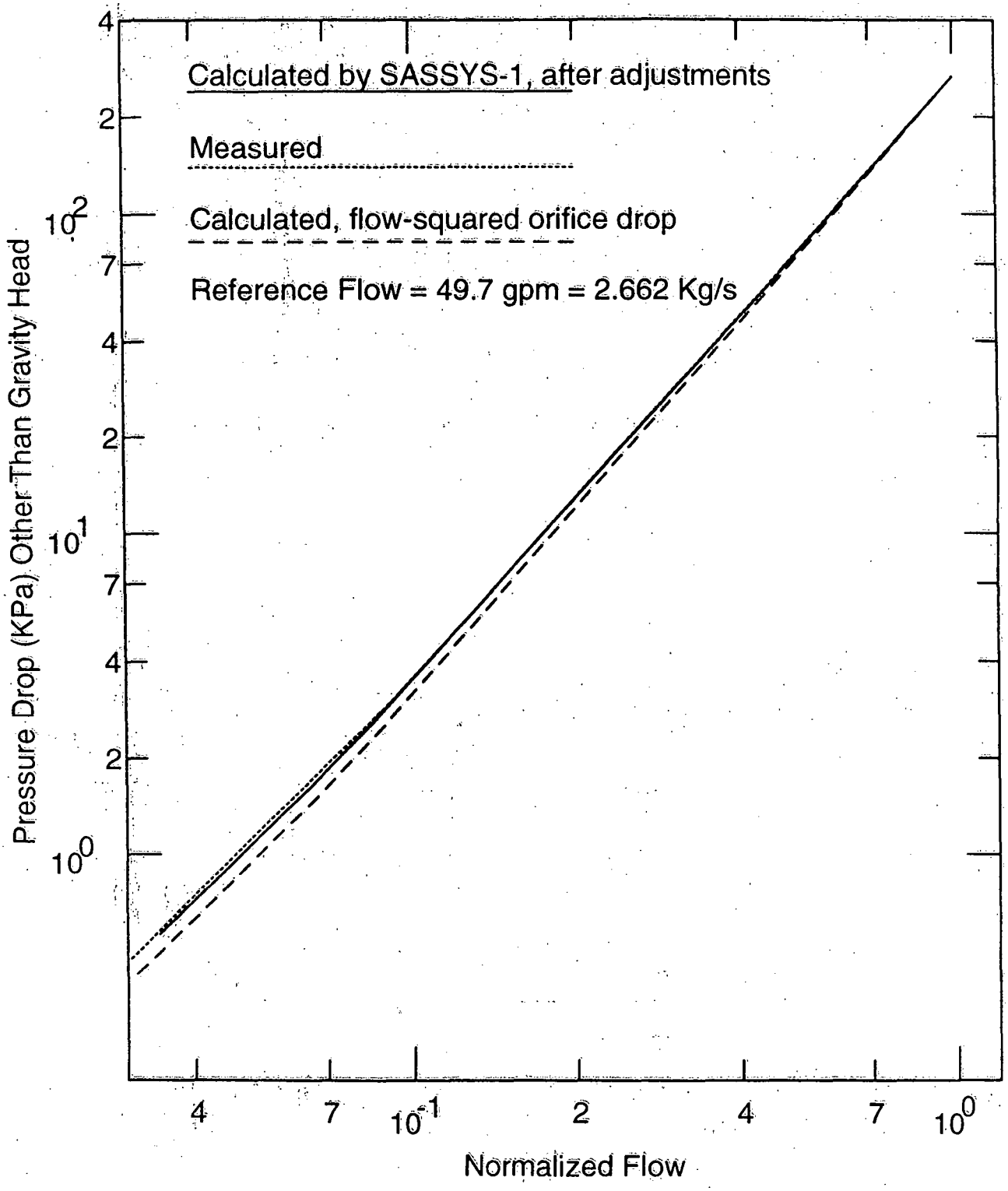

Figure 6. Isothermal Pressure Drop vs. Flow for XX09 at 800°F

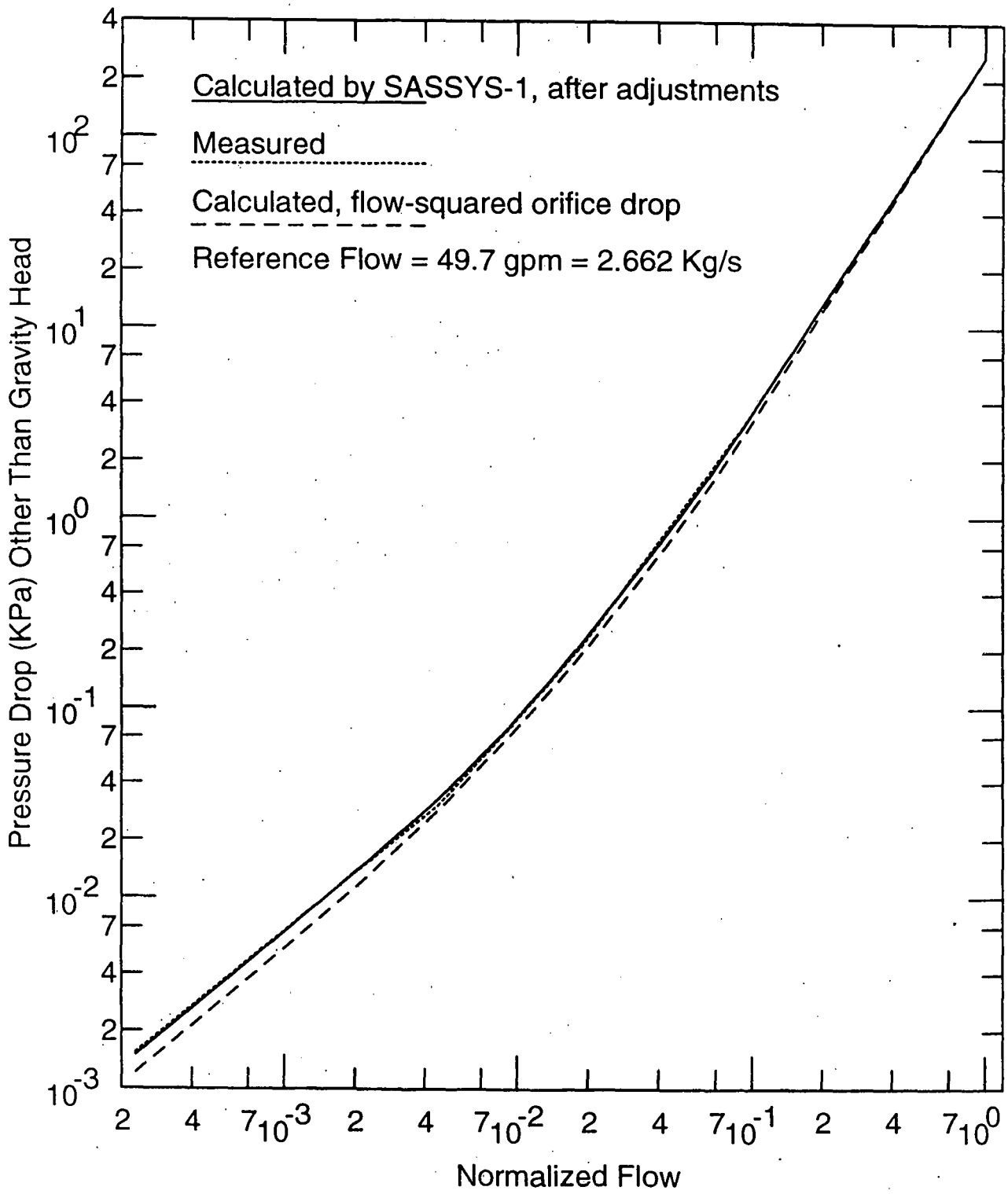

Figure 7. Isothermal Pressure Drop vs. Flow for XX09 at 800°F
Extended Range

where

S = spacing between pins

and

D = pin diameter.

The subchannel values had to be added in parallel and in series to obtain overall channel values. Also, a small correction was made to the thermal conduction terms to account for heat conduction through the pins. For the turbulent mixing term, the heat transfer coefficient between neighboring coolant subchannels was calculated as:

$$U_2 = \frac{C_T S}{A_i + A_{i+1}} \tag{59}$$

where

C_T = turbulent mixing coefficient

and

A_i = coolant flow area in channel i.

For these calculations, a value of .03 was used for the turbulent mixing coefficient, C_T. This value for C_T is consistent with the correlation of Cheng and Todreas,[24] which gives a value of .023 $\pm$25% for this case. Again subchannel values had to be added in parallel and in series to obtain overall channel values.

Table 2 lists the values of U_1 and U_2 used for these calculations.

Table 2 Coolant-to-Coolant Heat Transfer Coefficient Parameters

Channel	U_1	U_2
20	1.04	1.785
21	.41	.872
22	.36	.756
23	.34	.734

Note: See Equation 1 for the use of U_1 and U_2.

3.2 Results

Figure 8 shows the normalized power history used in these calculations, as well as the measured and computed normalized total flows for XX09. The pumps trip and start coasting down at time zero. Pump 1 stops at 100.6 seconds, and pump 2 stops at 91.9 seconds. Figure 9 shows the resulting coolant temperatures near the top of the core in XX09. The peak calculated temperature is for channel 24. The peak measured value is an average of the values for TTC30 and TTC31. The average values are weighted values, weighted by the number of pins per channel in the SASSYS-1 model.

The agreement between measured and calculated temperatures is remarkably good, especially considering the uncertainties in both the measurements and the calculations. These uncertainties include thermocouple calibration, thermocouple jitter, overall reactor power and flow, XX09 power and flow relative to the overall reactor values, uncertainties in model parameters, and the fact that bowing of the pins and the duct walls caused both initial distortions and transient distortions of the actual XX09 geometry from the perfect array of straight pins modeled in the calculations. To some extent, some of these uncertainties can be quantified. For instance, three different energy balances were made on the system before the start of the transient, giving three values that differ by 2-3%. Thus, the uncertainty in the power is at least 2-3%. A 1% change in power corresponds to a change of about 1 K in top of core coolant temperature at the start of the transient, or 3 K at the peak. Also, examination of the thermocouple data from before the start of the transient, when temperatures should have been constant or varying slowly and smoothly, shows that the jitter in the readings for most thermocouples was 1 K or less; but the readings for TTC 34 varied within a range of more than 4 K; and the readings for TTC 35 varied within a range of more than 2 K. Thus, thermocouple jitter probably contributes at least 1 K to the uncertainties. The difference between calculated and computed initial temperatures is 5-8 K. This difference is probably within the calibration uncertainty of the thermocouples. Alternatively, a 5% change in power or flow in XX09 would account for this difference. Figure 10 shown the results of increasing the computed initial flow rate by 5% in XX09, adjusting the inlet orifice to match overall pressure drops, and then

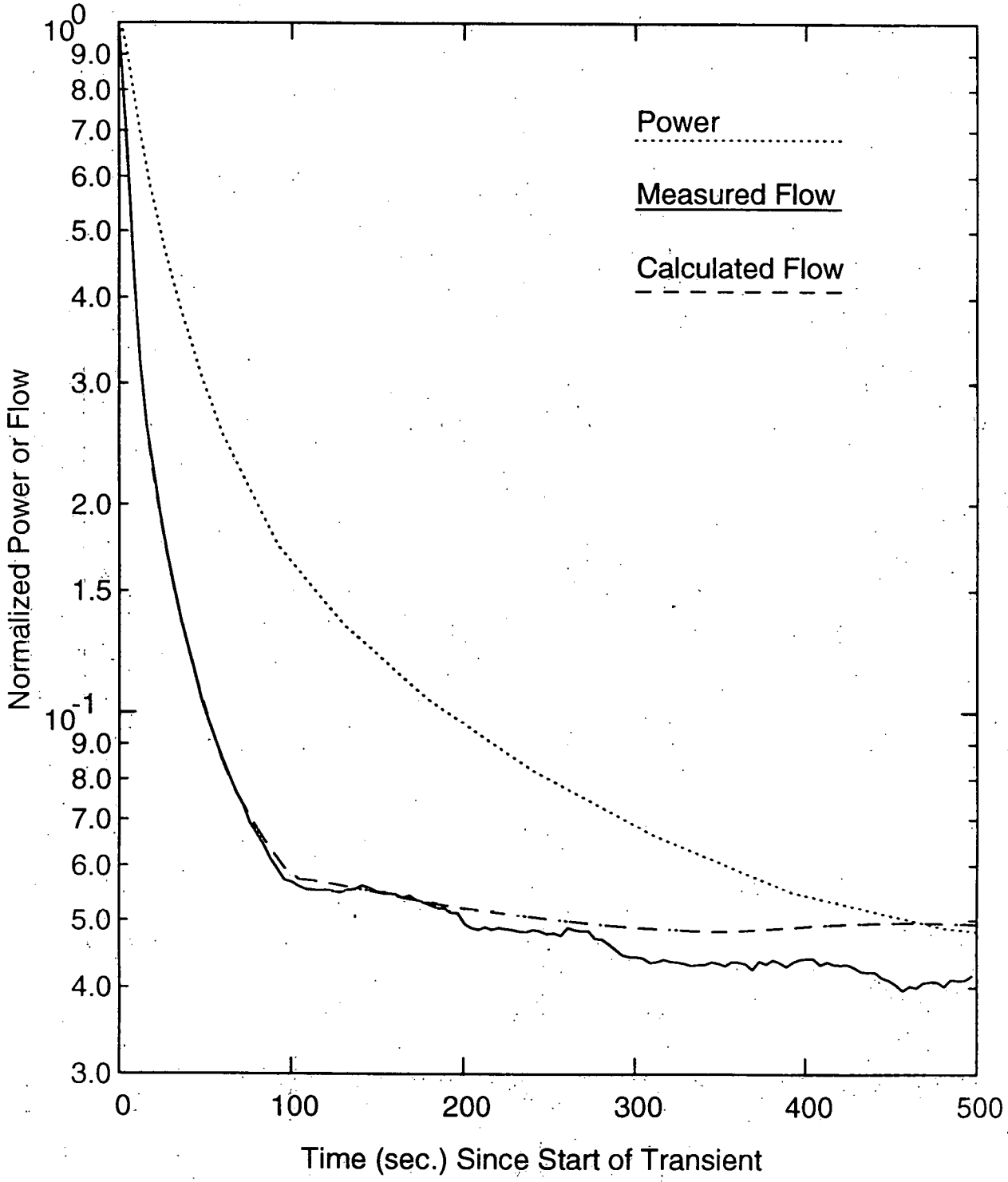

Figure 8. SHRT 45 Power and Flow

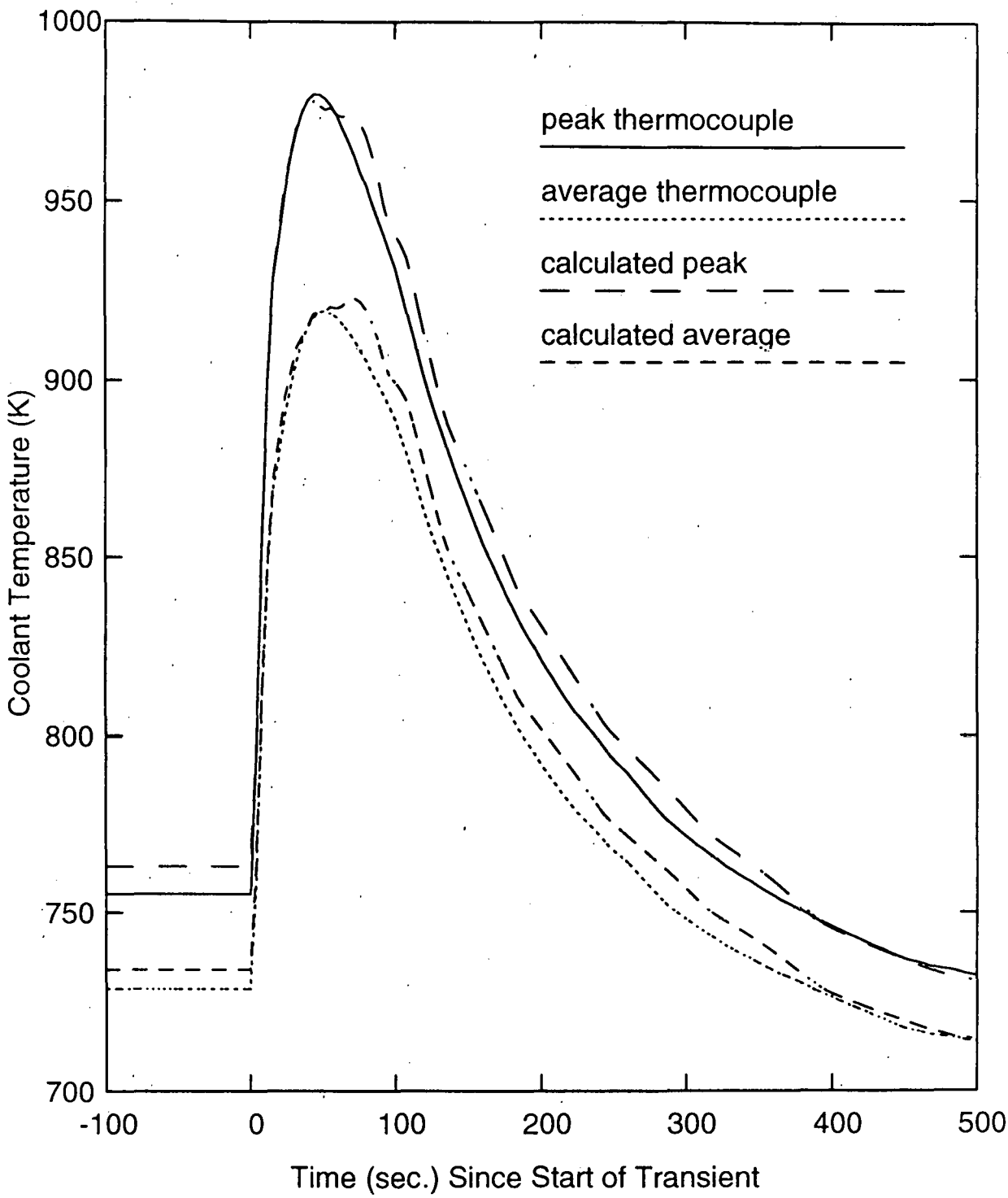

Figure 9. SHRT45 Top of Core XX09 Coolant Temperatures

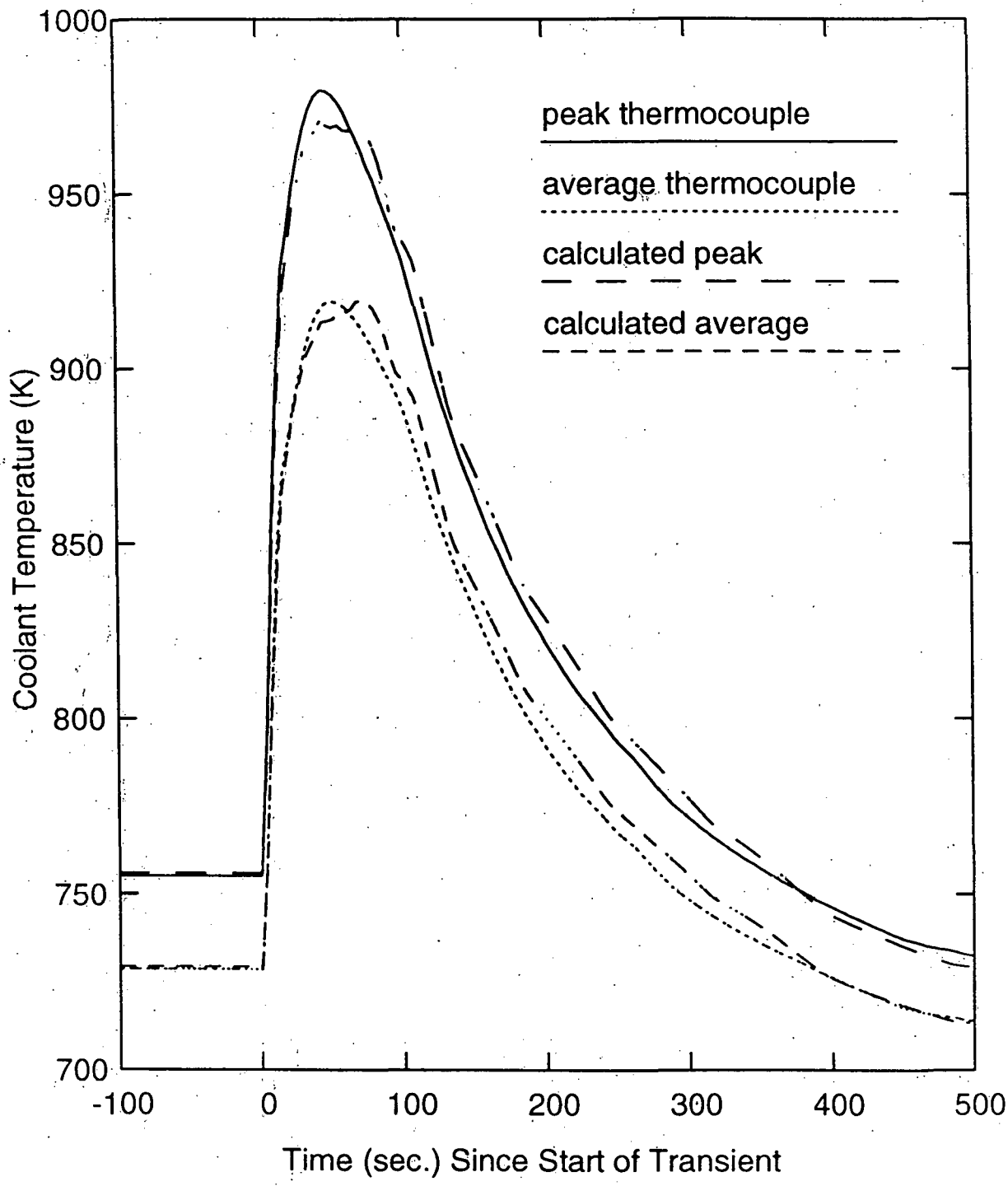

Figure 10. SHRT 45 Top of Core XX09 Coolant Temperatures, 5% Extra Flow

running the same transient. Other than geometry distortions due to bowing or shifting of pins, probably the largest modeling uncertainties are in the parameters for coolant-to-coolant heat transfer. An exact value for the turbulent coefficient U_2 can not be obtained from theoretical considerations, especially when the contribution of the wire wrap is included. On the other hand, the thermal conduction shape factor U_1 of Equation 58 is based on electrical analog measurements. In principle, U_1 could also be calculated from detailed two-dimensional thermal conduction calculations.

Figure 11 shows the computed transient flow redistribution for the center channel (channel 24). As the flow drops during the transient, buoyancy effects become more important, and the flow in the hotter center channel increases relative to the average. The coolant temperature peaks at about 50 seconds, whereas the flow redistribution does not peak until the pumps stop at 90-100 seconds. At 50 seconds, flow redistribution added only about 8% to the center channel flow, corresponding to a change of about 28 K in peak temperature. At this point, the difference between the peak and average temperatures was 58 K, so transient flow redistribution reduced the peak-to-average temperature difference by almost 50%. At 100 seconds, the change in center channel flow was about 13.8%, corresponding to a change of about 45 K in peak temperature.

Figure 12 shows a comparison between calculated and measured individual thermocouple temperatures across the subassembly, from corner to corner, at one time during the transient. The computed and measured temperatures have very similar shapes, but the measured values reflect some non-symmetric effects that are not accounted for in the concentric ring representation used for the calculations. One non-symmetric effect is a power skew across the subassembly: the power is highest in the direction toward the center of the core, leading to a non-symmetric temperature distribution. Another effect is bunching of the pins; the pin bundle is apparently tighter in the vicinity of thermocouples 30 to 33 than on the other side of the subassembly near thermocouples 28 and 29. The bunching in the center near thermocouples 30 and 31 is accounted for in the calculation, but non-symmetric bunching near locations 32 and 33 is not accounted for.

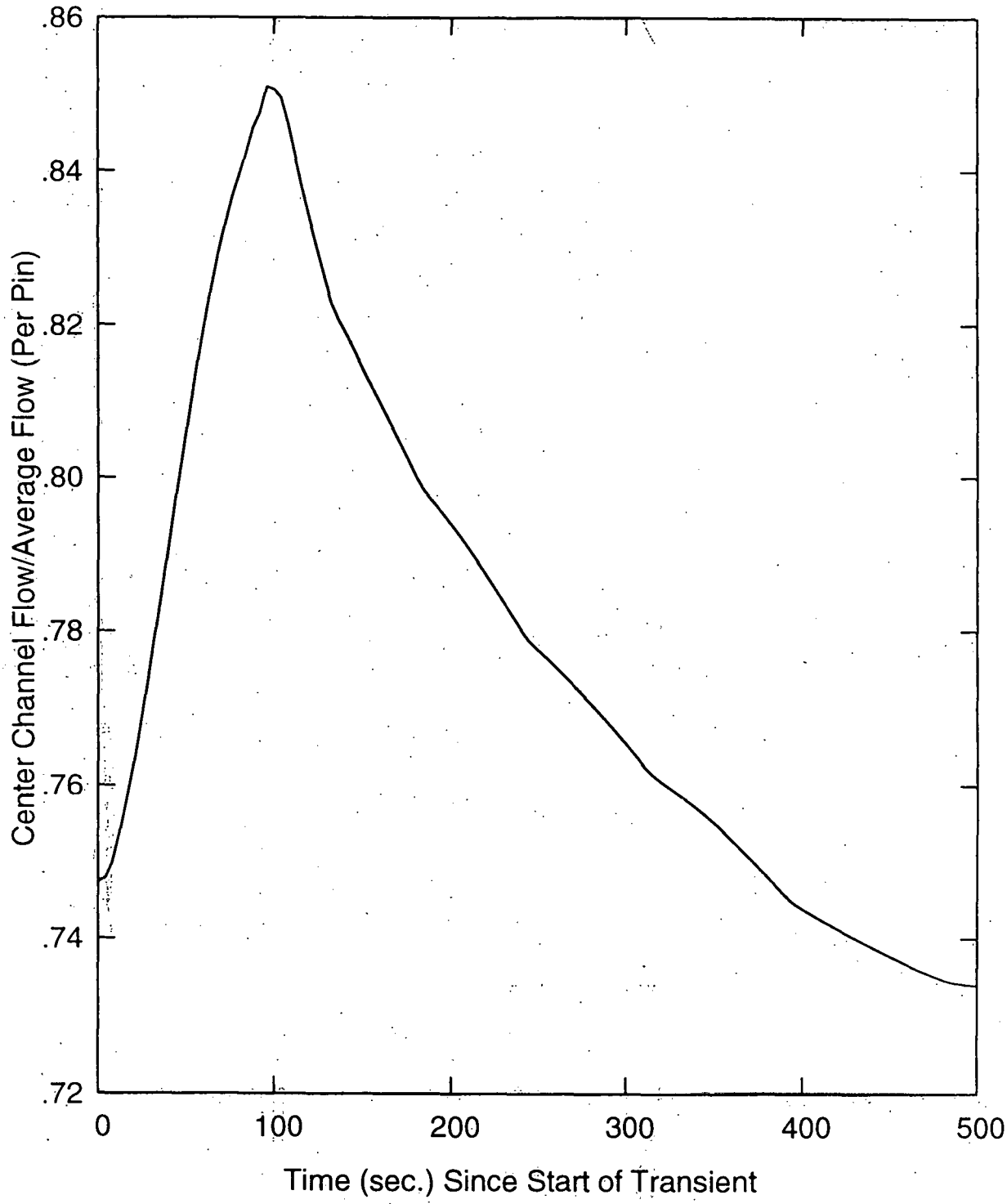

Figure 11. SHRT45 Transient Flow Redistribution

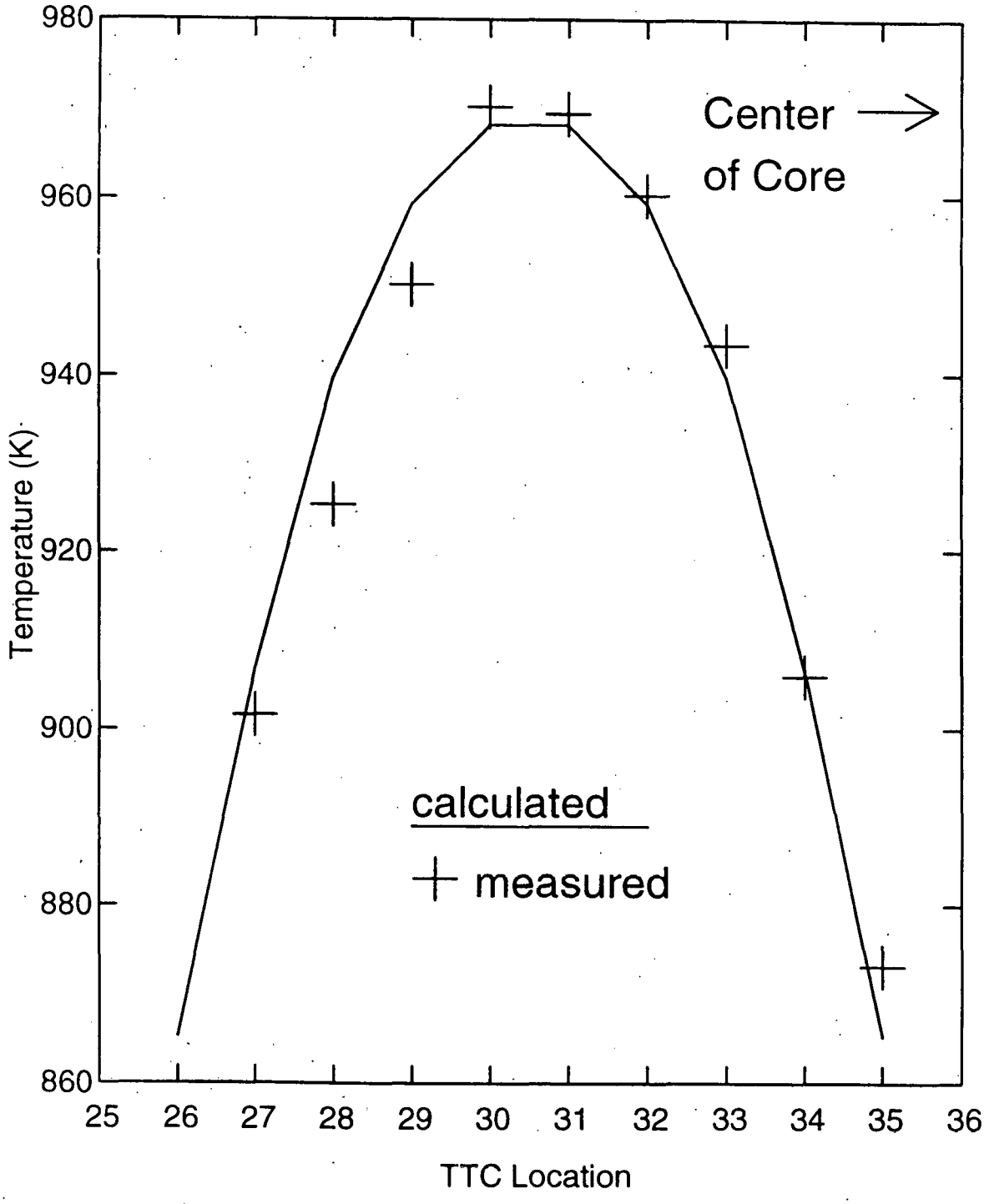

Figure 12. SHRT-45 Detailed Thermocouple Comparisons, t = 64 sec.

In addition to the top of core temperatures mentioned above, temperaure data is also available from the 14TC thermocouples located 14 cm above the top of the core in XX09. Figure 1 shows the locations of these thermocouples. Comparisons between measured and computed temperature for these thermocouples are shown in Figures 13-15. The computed values in these figures are for the case with 5% extra coolant flow. The computed temperatures agree well with the measured values except for the initial temperatures at the edge of the subassembly. The initial edge temperature measured by 14TC 43 was probably influence by bowing that tightened the pin bundle in the vicinity of this thermocouple. 14TC 43 is near the edge thermocouple TTC 35 at the top of the core. Before the start of the transient, TTC 35 read higher than TTC 34; but by four seconds into the transient, TTC 35 read lower than TTC 36 and stayed lower for the rest of the transient. Apparently, the pin bundle in the vicinity of TTC 36 and 14TC 43 was initially tighter than nominal before the start of the transient; and it loosened during the transient.

In addition to the XX09 thermocouple data, there is also SHRT-45 flowmeter data, both for XX09 flow and for system flows. The flowmeter data poses special problems, in terms of agreement between different flowmeters that are measuring the same flow, in terms of initial steady-state normalization, in term of the accuracy or reliability of the relative transient values, and in terms of consistency between measured flows, powers, and temperatures.

There are two flowmeters in series in XX09. They give readings that differ by a factor of four, so at least one of them is wrong. The upper flowmeter reading for the initial steady-state flow is 14% less than the computed value given in reference 15, so the upper flowmeter may have been working moderately well, at least at higher flow rates. Therefore, the lower flowmeter data was ignored, and all measured XX09 flows presented in this report are from the upper flowmeter. As shown in Figure 8, at higher flows, the measured and calculated normalized flows for XX09 agree quite well. At low flows the flowmeter readings show a lot of random fluctuations, and they are probably not reliable. Another XX09 flowmeter issue is calibration on normalization. Figure 16 shows the temperatures computed when the initial XX09 flowrate was reduced by 14% to agree with the upper flowmeter, and the XX09 power was reduced by 18% so that the initial top of core coolant temperatures would agree with the

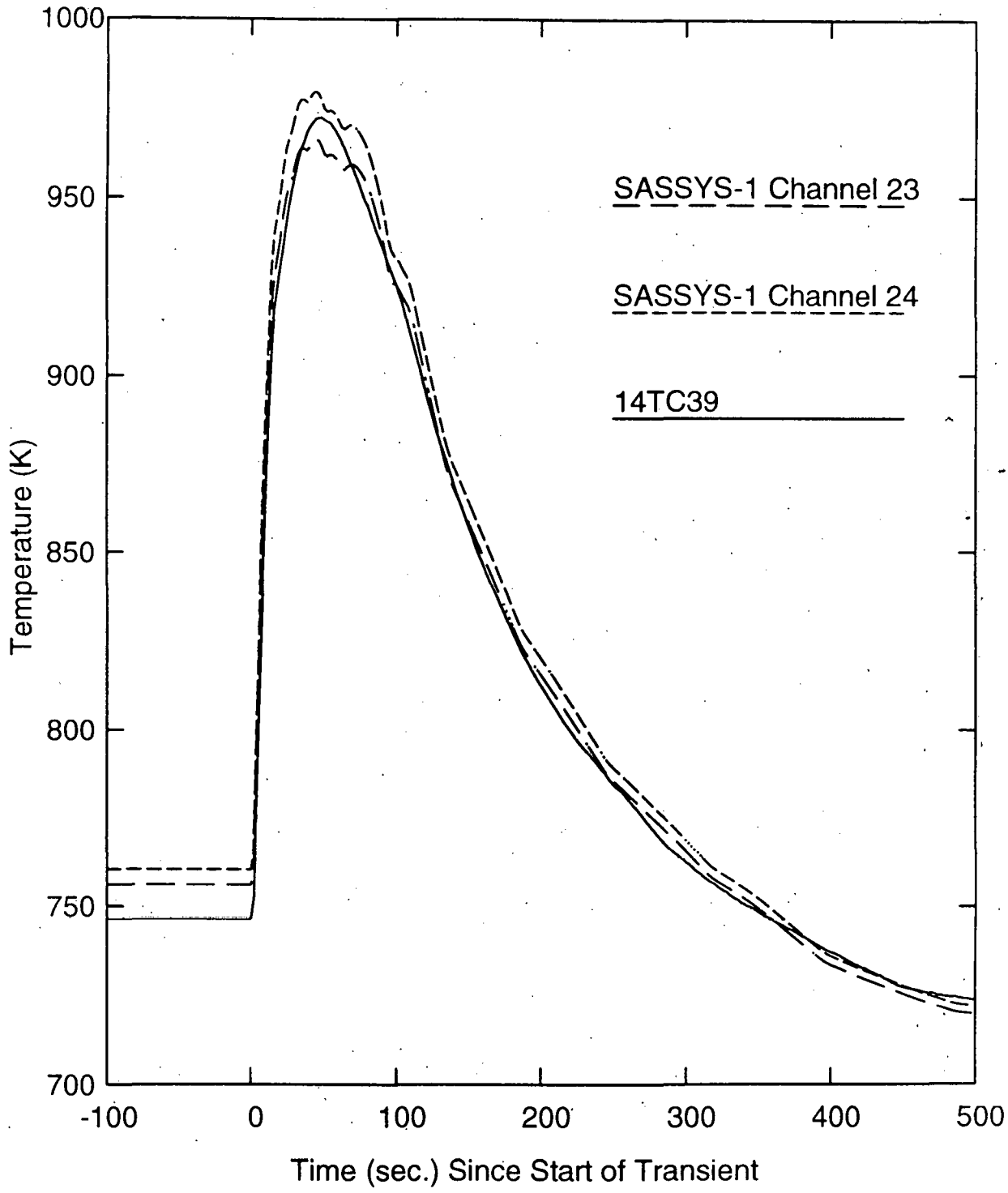

Figure 13. SHRT-45 XX09 Above-Core Temperature, 5% Extra Flow, Inner Channel

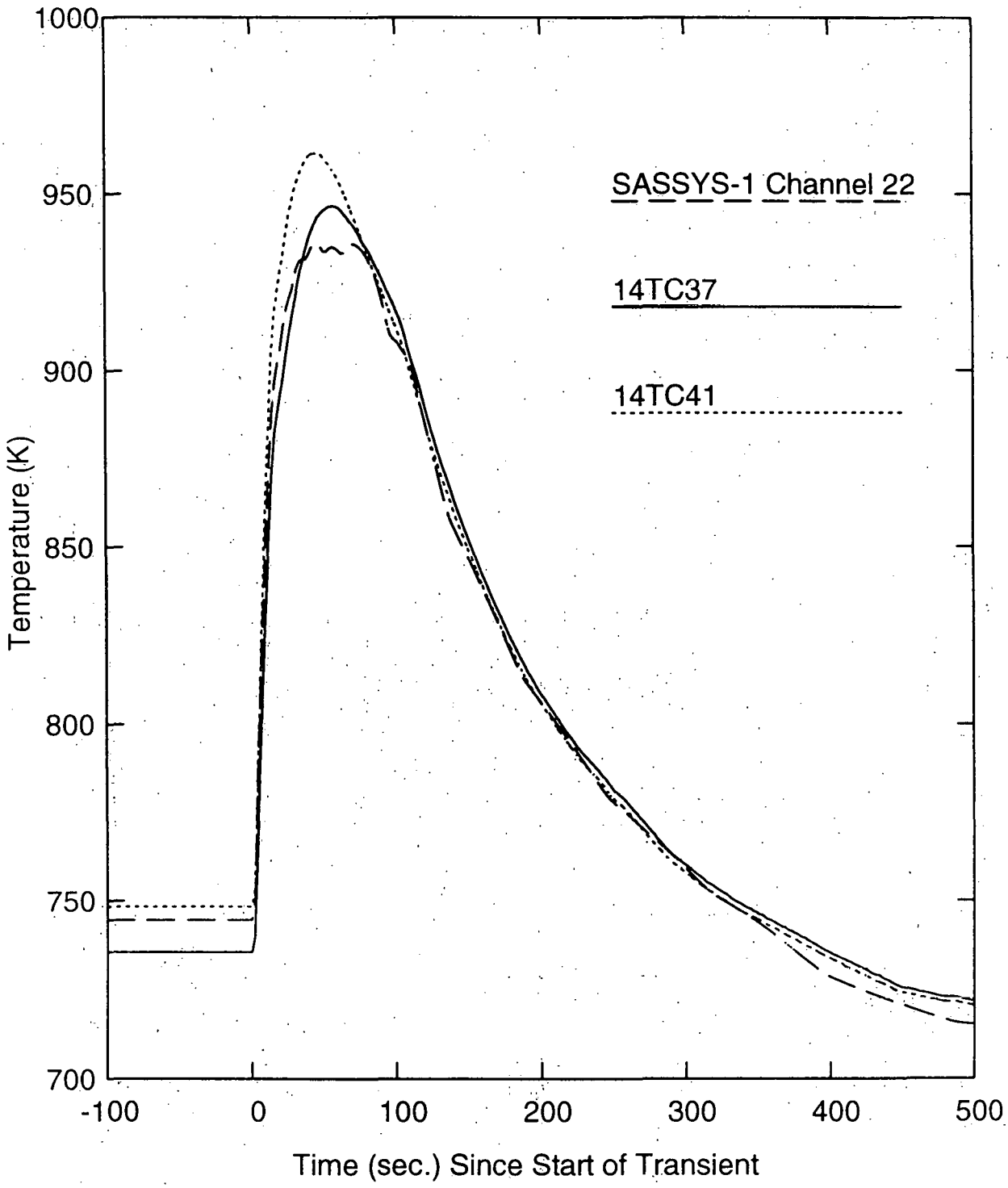

Figure 14. SHRT-45 XX09 Above-Core Temperature, 5% Extra, Flow, Middle Channel

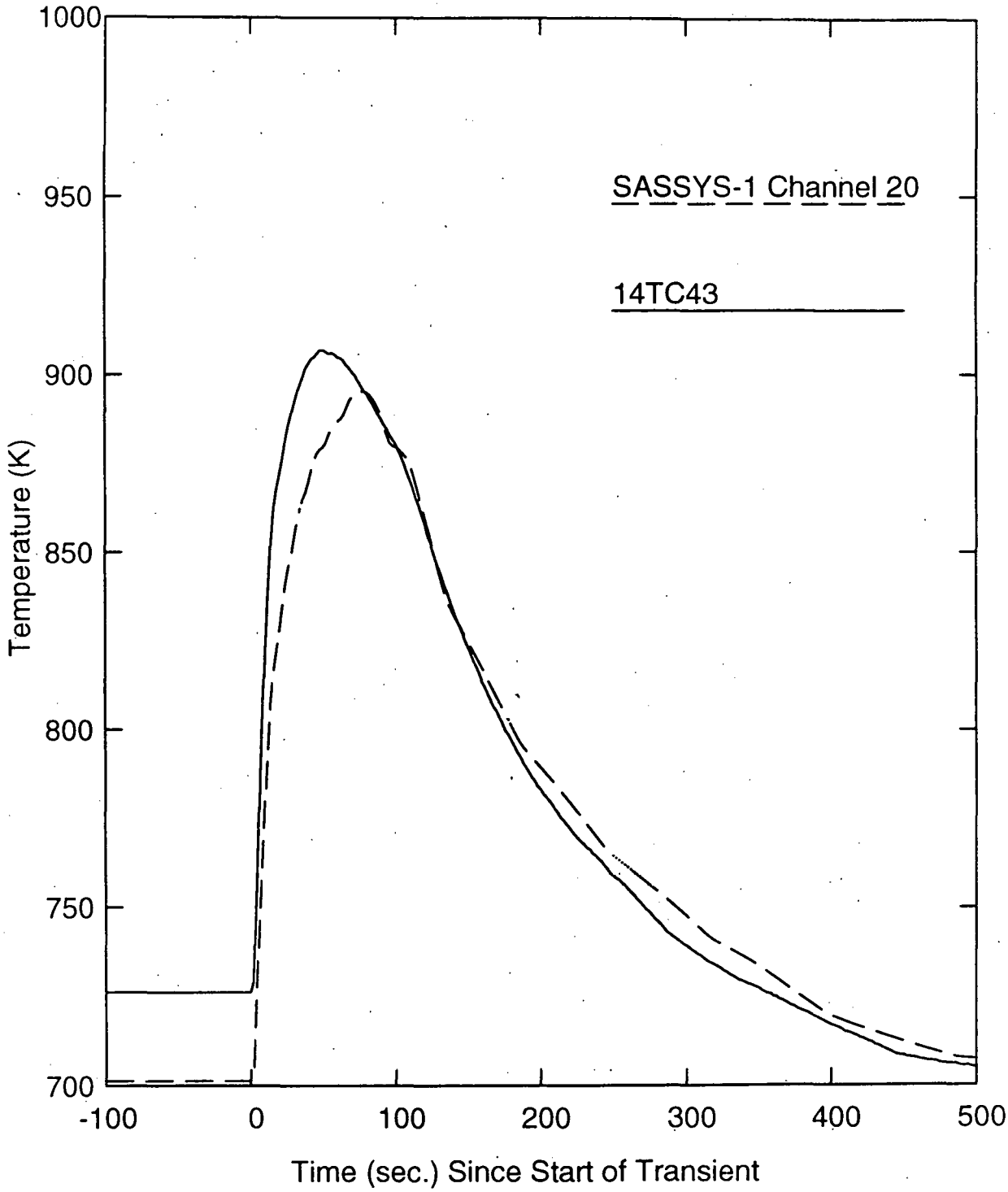

Figure 15. SHRT-45 XX09 Above-Core Temperature, 5% Extra Flow, Edge Channel

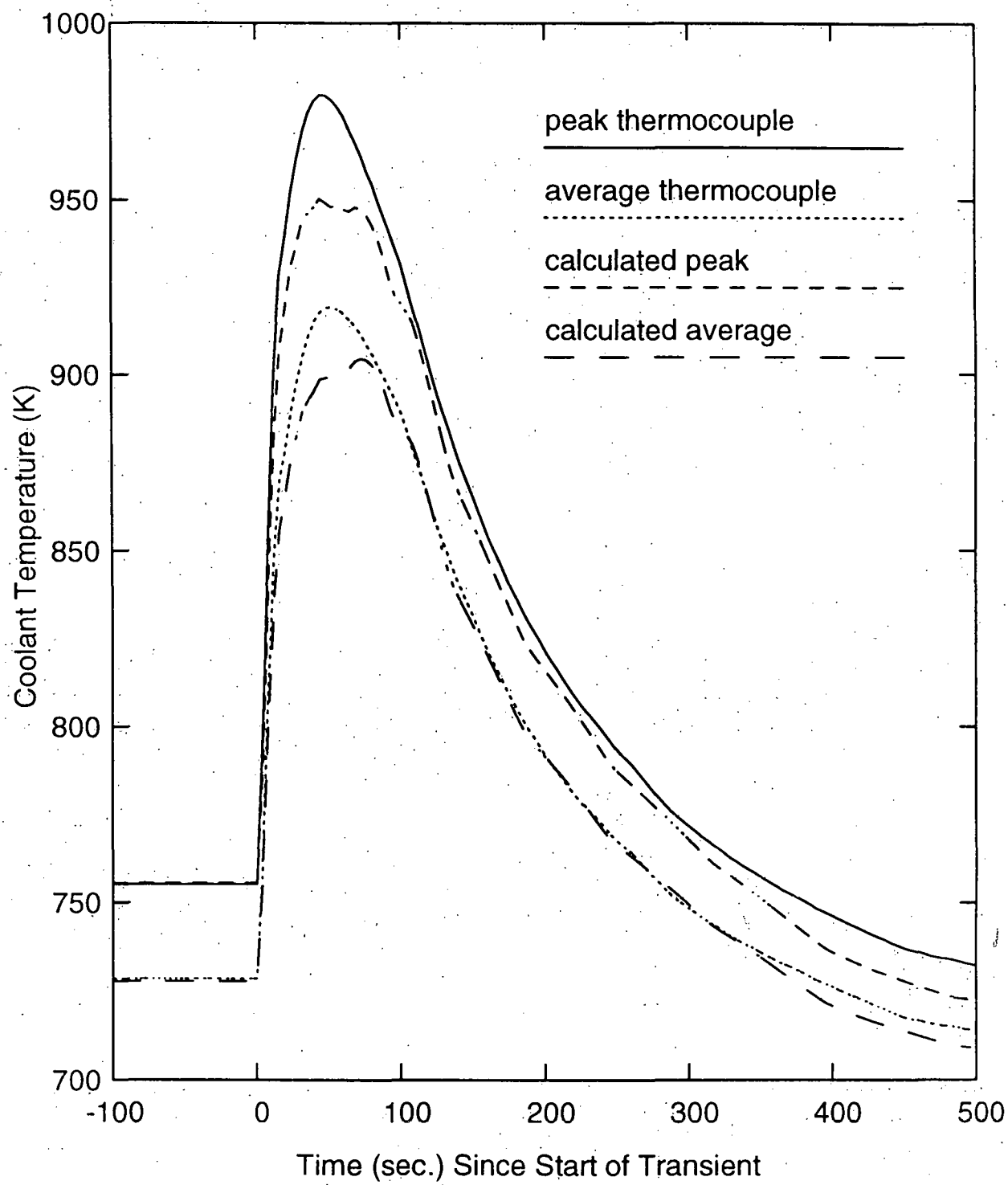

Figure 16. Top of Core XX09 Temperature, 14% Less Flow

measured values. Powers and flows in the rest of the reactor were left unchanged for this calculation. In this case, with the initial XX09 coolant flow set equal to the flowmeter value, the agreement between calculated and measured transient coolant temperatures is significantly poorer than in the cases shown in Figures 9 and 10, with the initial XX09 coolant flow determined by EBRFLOW or the EBRFLOW value plus 5%. Figure 17 shows the normalized flowrates for these three cases. After normalizing to the steady-state value, the transient flowrates are relatively insensitive to the initial value; but again the EBRFLOW case or the EBRFLOW +5% case agrees with the transient measurements better than the case using the measured initial flowrate. On the basis of the transient temperature results, it appears that the EBRFLOW value for the initial flowrate is closer to the real value than the flowmeter value is.

There are four operational primary system flowmeters in EBR-II: an EM flow meter between pump 2 and the high pressure inlet plenum, an EM flowmeter between pump 2 and the low pressure inlet plenum, and two outlet plenum flowmeters. The SASSYS-1 primary loop input was set up so that the initial steady-state flows agreed with the measured values for these four flowmeters. Figures 18 and 19 show the calculated and measured transient primary system flowrates. The outlet plenum flowmeters are not considered to be reliable or accurate at lower flows, so it is no surprise that the measured values differ significantly from each other and from the calculated values at lower flowrates. On the other hand, it is hoped that the EM flowmeters are reasonably accurate at low flows, and the computed and measured pump 2 to high pressure inlet plenum flows agree to within about 10% for the first 250 seconds of the transient. After that, the measured values drift lower with a fair amount of noise in the signal.

In summary, at the 20% uncertainty level everything in the SHRT-45 analysis holds together: the measured temperatures are consistent with the measured powers and flows, and the calculated temperature and flowrates agree with the measured values where the measurements are considered to be reliable. Note that the initial steady-state coolant temperature rise across the core in XX09 is about 100 K, whereas at the time of the temperature peak the temperature rise is about 300 K. Therefore, a 1% change in power or flow corresponds to a temperature

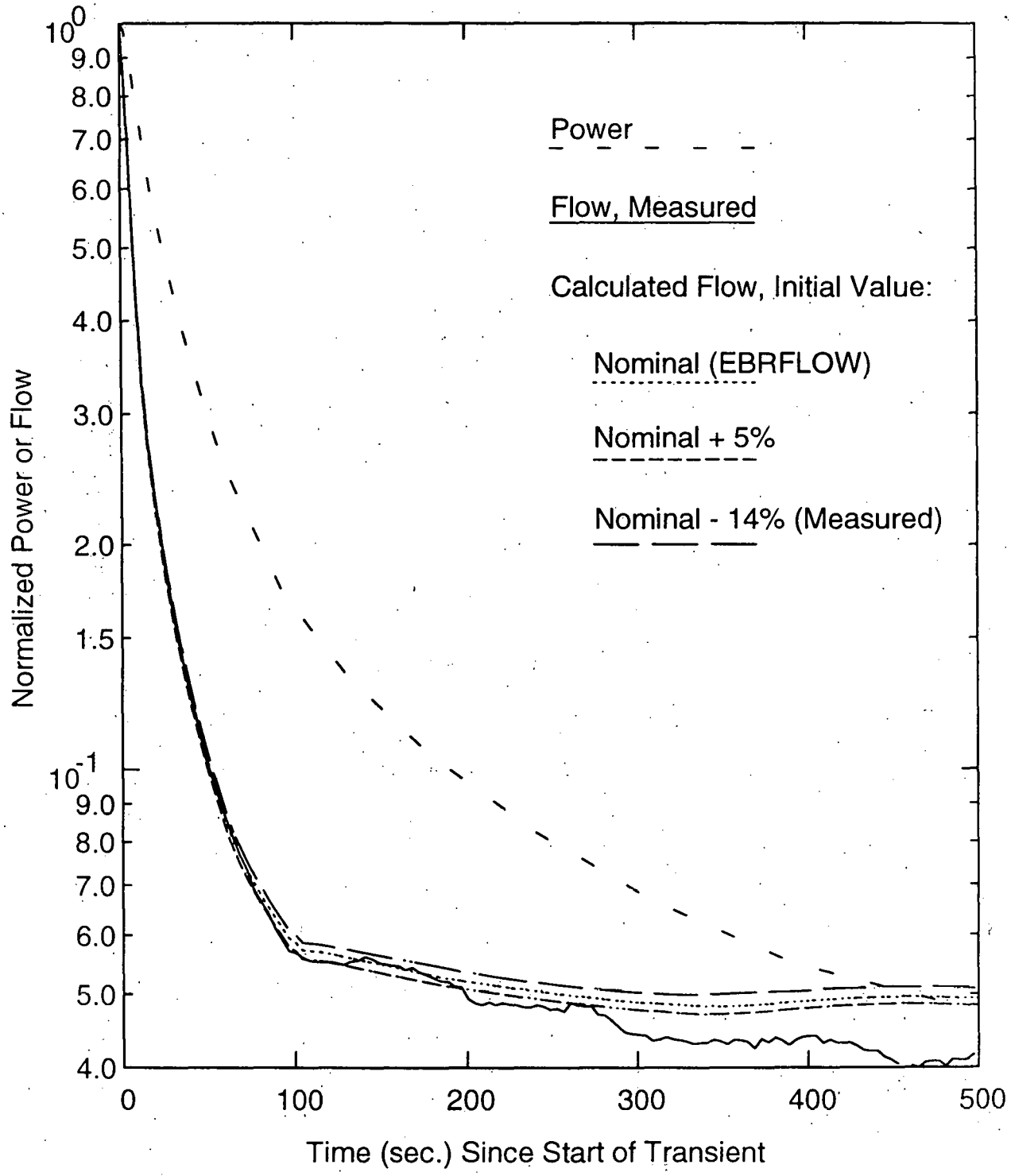

Figure 17. SHRT-45 XX09 Flow Rate Comparisons

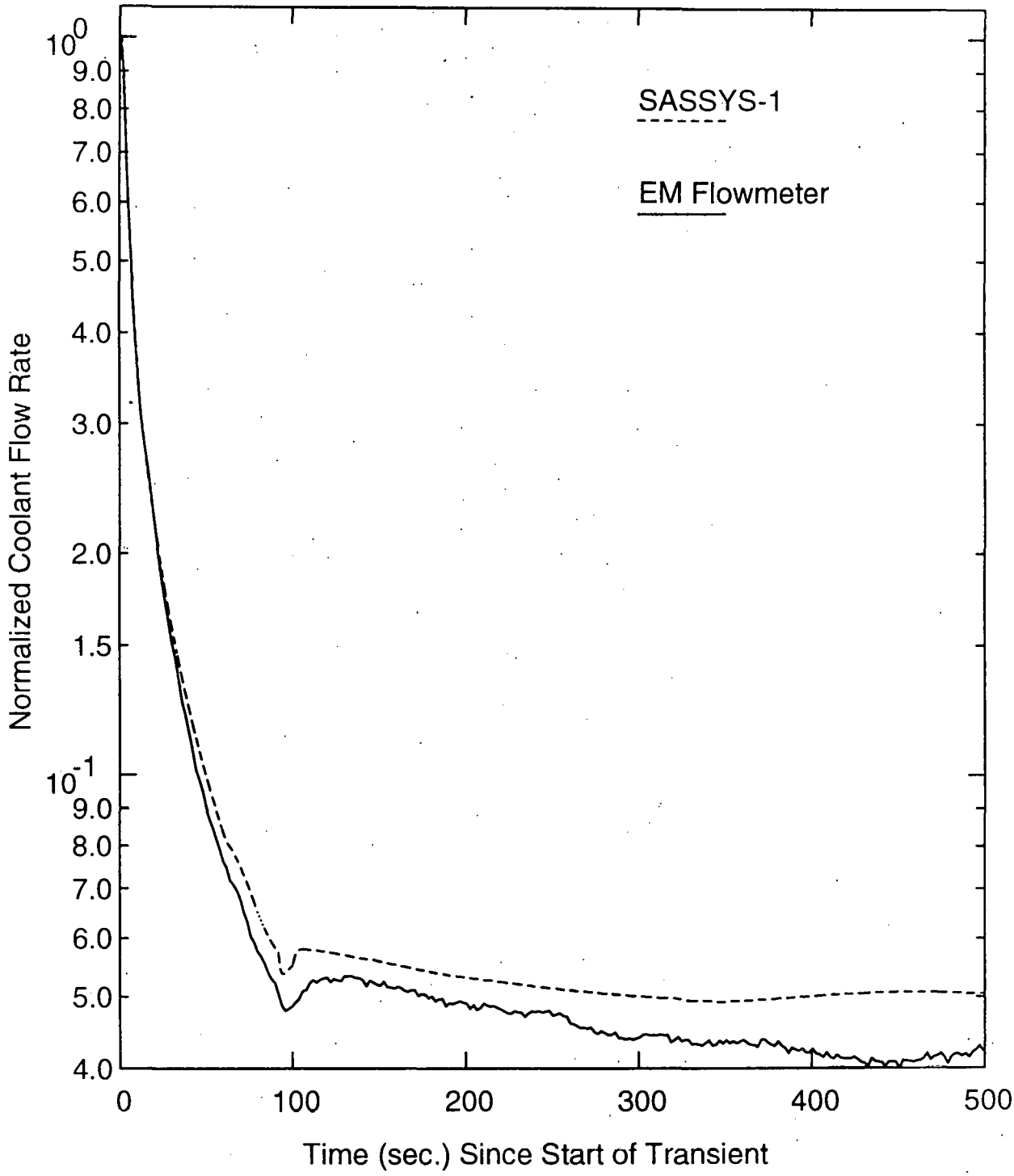

Figure 18. Pump 2 to High Pressure Inlet Plenum Flow Rates

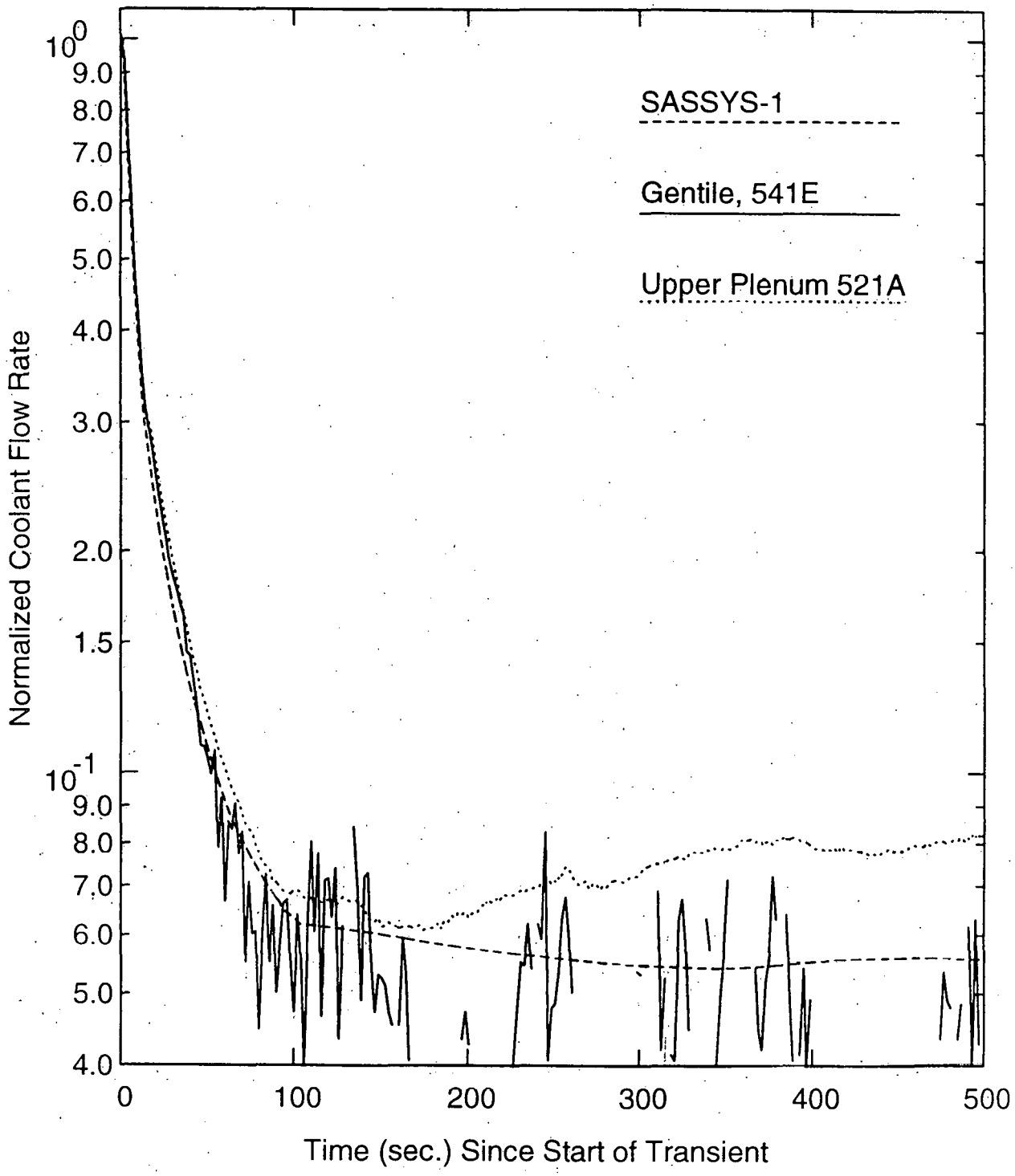

Figure 19. Outlet Plenum Flow Rates

change of about 1 K at the start of the transient, or 3 K at the temperature peak. At the 10% uncertainty level, some differences appear between measured and computed flowrates; and there are some difficulties in obtaining consistency between measured temperatures and measured powers and flows. The agreement between calculation and measurement is better for temperatures than for coolant flowrates: most temperatures agree to within 5% or better.

3.3 Assessment of Results

The two main aspects of computing accurate temperatures for a case like this are getting the time-dependent average temperature right and getting the correct peak-to-average temperature difference. The peak-to-average temperature difference is determined mainly by the transient channel-to-channel flow distribution and the channel-to-channel heat transfer coefficients. On the other hand, the average temperature is determined mainly by the power level, the average coolant flow rate, and the heat flow to the thimble flow region and to neighboring subassemblies. In turn, the average coolant flow rate is determined mainly by the pressure drop vs. flow characteristics of the subassembly and by the pump head vs. flow and speed characteristics of the primary pumps, as well as the total coolant flow through the pumps. In the later parts of the transient, gravity heads in the whole primary system also have a large effect on coolant flows. Note that the earlier parts of this transient involve forced convection and turbulent flow, whereas the later parts involve natural circulation and laminar flow. In order to obtain the good agreement between measured and computed temperatures indicated in Figure 6, all of these factors must be computed fairly accurately. Thus, these calculations provided a test of not only the new multiple pin model, but also of the overall thermal hydraulic modeling of the whole primary coolant system.

4.0 MODEL ASSESSMENT

This new multiple pin model has some large advantages, as well as some definite limitations. One limitation is that it is basically a two dimensional (r-z) model. A good analysis of a subassembly with a strong side-to-side power skew plus the normal overcooling of the edge pins would probably require a model in which coolant in channel i communicates with more than just

channels i-1 and i+1. Such a capability may be added to the code in the future. Another limitation is that since there is no cross-flow between channels in the pin section the model can not analyze an internal flow blockage. An important limitation of this model is that it only handles single phase coolant and no pin failure or pin disruption. Thus, it can not handle either severe accidents or the analysis of voiding due to gas release from pin failures as described in reference 25. Finally, the explicit forward time differencing treatment of the subassembly-to-subassembly heat transfer and the heat transfer to the thimble flow region limit the maximum time step size that can be used, and thereby limit the computational speed. For the SHRT-45 analysis, a time step size of .2 seconds was used; whereas time steps of 1 second or larger are often used for SASSYS-1 runs; and time steps as large as 16 seconds have been used. If the detailed steam generator model is used, the time step size used for the core channel analysis does not matter very much; since the detailed steam generator calculations and possibly some of the balance-of-plant calculations can dominate the computation time. On the other hand, SASSYS-1 cases, including this one, are often run with a simple steam generator model; and then the core channel time step size determines the computation time. The SHRT-45 case ran 1.5 times as fast as real time on a Cray XMP computer, whereas the SASSYS-1 shut-down heat removal case reported in reference 26 ran 180 times as fast as real time on the same computer. Since shut-down heat removal cases sometimes involve transients lasting for days, a very rapid computational speed is desirable for such cases. If such cases are to be run routinely with subassembly-to-subassembly heat transfer in SASSYS-1, then the code will probably have to be modified to solve for temperatures in all interacting subassemblies simultaneously. Note that this time step limitation does not apply to the multiple pin treatment within a subassembly; only the subassembly-to-subassembly or the subassembly-to-thimble flow region calculations are numerically unstable with large time step sizes.

The new multiple pin model has some tremendous advantages. It allows SASSYS-1 to calculate accurate time dependent peak temperatures mechanistically in addition to the average temperatures the code previously calculated. For many uses, peak temperatures are of more interest than average temperatures. Another advantage is that the peak temperature calculation is part of an integrated, single code approach to the whole problem. Also, even with the time step limitations imposed by the subassembly-to-subassembly heat transfer calculations, the

multiple pin analysis still runs fast enough to be used for routine analysis in most cases. Finally, a very important consideration is that the detail provided by the multiple pin model makes it possible to make detailed comparisons with experimental data at a level never before possible with the code. Previously, a temperature calculated for an average pin could be compared with thermocouple data; but the fact that the computed data fell somewhere within the range of the various thermocouples could mask significant model limitations. Being able to calculate the temperatures seen by individual thermocouples gives a much better indication of the adequacy of the modeling. Also, having the total calculation in a single integrated code provides much better model validation than having the hot channel analysis in one code and the rest of the analysis in one or two other codes. Discrepancies between calculated and measured values can not be blamed on errors in another code or on inadequate coupling between codes. On the other hand, errors in other codes or inadequate coupling between codes do not confuse the issue and indicate poor agreement in cases where the hot channel analysis itself is adequate. Thus, an integrated treatment allows one to concentrate on the real modeling issues. Another aspect of model validation or verification is that even with subassembly-to-subassembly heat transfer, the code runs fast enough that for a given experiment it is feasible to run many calculations exploring the influence of variations in model parameters or the use of different models.

5.0 CONCLUSIONS

A multiple pin treatment has been added to SASSYS-1 in order to calculate pin-to-pin and coolant subchannel-to-coolant subchannel temperature distributions. Computed transient peak and average coolant temperatures agree well with XX09 thermocouple data from the SHRT-45 test in EBR-II; indicating that not only are the intra-subassembly effects handled well, but the whole primary coolant system is modeled well. The new multiple pin treatment provides a way to compute accurate time-dependent peak temperatures within the framework of a single unified code. The new treatment also makes possible exact comparisons with detailed experimental data.

There are a couple of additional conclusions from the SHRT-45 analysis. One conclusion is that local bunching of pins due to bowing or shifting is an important contribution to

temperature peaking: an analysis of a subassembly with uniformly spaced pins with nominal pitch will often under-predict the peak temperature. Another conclusion is that the EBRFLOW prediction for the steady-state coolant flow in XX09 in this test appears to be more accurate than the flowmeter reading, which was 14% lower.

6.0 ACKNOWLEDGEMENTS

The author wishes to thank Earl Feldman and Dale Mohr, who provided the experimental data from the SHRT-45 test, as well as numerous discussions about EBR-II in general and the test in particular.

REFERENCES

1. F. E. Dunn, F. G. Prohammer, D. P. Weber, and R. B. Vilim, "The SASSYS-1 LMFBR Systems Analysis Code," ANS International Topical Meeting on Fast Reactor Safety, Knoxville, TN, pp. 999-1006 (April 1985).

2. P. A. Pizzica, "An Improved Steam Generator Model for the SASSYS Code," Trans. Am. Nucl. Soc., 60, 712 (1989).

3. Laural L. Briggs, "A New Balance-of-Plant Model for the SASSYS-1 LMR Systems Analysis Code," Trans. Am. Nucl. Soc., 60, 709 (1989).

4. J. Y. Ku, "SASSYS-1 Balance-of-Plant Component Models for an Integrated Plant Response," Trans. Am. Nucl. Soc., 60, 716 (1989).

5. R. B. Vilim, T. Y.C. Wei, and F. E. Dunn, "Generalized Control System Modeling for Liquid-Metal Reactors," Nucl. Sci. and Eng., 99, 183 (1988).

6. William T. Sha, Frank J. Goldner, Paul R. Huebotter, and Robert C. Schmitt, "Thermal Hydraulic Multichannel Analysis," Proceedings of the International Meeting on Reactor Heat Transfer, Karlsruhe, Germany, p. 180, October 9-11, (1973).

7. Dale Mohr, Lu-Kang Chang, and H. P. Planchon, "Validation of the HOTCHAN Code for Analyzing the EBR-II Core Following an Unprotected Loss of Flow", Trans. Am. Nucl. Soc., 57, 318, (1988).

8. [redacted]

9. H. P. Planchon, R. M. Singer, D. Mohr, E. E. Feldman, L. K. Chang, and P. R. Betten, "The Experimental Breeder Reactor II Inherent Shutdown and Heat Removal Tests - Results and Analysis," Nucl. Eng. and Design, 91, 287 (1986).

10. G. H. Golden, H. P. Planchon, J. J. Sackett, and R. M. Singer, "Evolution of Thermal Hydraulics Testing in EBR-II," Nucl. Eng. and Design, 101, 3 (1987).

11. D. Mohr, L. K. Chang, E. E. Feldman, P. R. Betten, and H. P. Planchon, "Loss-of-Primary-Flow-Without-Scram Tests: Pretest Predictions and Preliminary Results," Nucl. Eng. and Design, 101, 45, (1987).

12. F. E. Dunn and D. J. Malloy, "LMR Centrifugal Pump Coastdowns," Proceedings of an International Conference on Anticipated and Abnormal Transients in Nuclear Power Plants, Atlanta, Georgia p. VIII-21, April 12-15, (1987).

13. E. B. Wylie and V. L. Streeter, Hydraulic Transients; Chapter Nine, McGraw-Hill, New York, 1967.

14. E. B. Wylie and V. L. Streeter, Fluid Transients; Chapter Six, McGraw-Hill, New York, 1978.

15. K. E. Phillips to G. H. Golden, "Neutronics and Hydraulic Information for EBR-II Run 137E (SHRT) Loading," ANL EBR-II Memo, March 6, 1986.

16. J. Poloncsik, E. C. Filewicz, G. J. Kamis, and J. T. Natoce, "The Experimental Breeder Reactor II (EBR-II) Instrumented Subassemblies, Inset XX09 and XX10," Proceedings of the Conference on Fast, Thermal, and Fusion Reactor Experiments, Salt Lake City, Utah, American Nuclear Society, pp. 1-276 to 1-287, April 12-15, (1982).

17. Decay Heat Power in Light Water Reactors, American Nuclear Society, ANSI/ANS-5.1-1979.

18. E. H. Novendstern, "Pressure Drop Model for Wire-Wrapped Fuel Assemblies," Trans. Am. Nucl. Soc. 14, 660 (1971).

19. L. F. Moody, Mech. Eng. 69, 1005 (1947).

20. F. C. Engel, R. A. Markley, and A. A. Bishop, "Laminar Transition, and Turbulent Parallel Flow Pressure Drop Across Wire-Wrap-Spaced Rod Bundles," Nuclear Science and Engineering, 69, 290, (1979).

21. Jim Wendte, "Normal and Reverse Flow Tests on XX09, Including Low Flow" ANL EBR-II Intra-Laboratory Memo, August 4, 1982.

22. J. C. Wendte, "Flowhole Sizes in XX09 Lower Adapter" ANL EBR-II Intra-Laboratory Memo, September 12, 1980.

23. A. Fukuda, Oak Ridge National Laboratory, personal communication (1972).

24. Shih-Kuei Cheng and Neil E. Todreas, "Hydrodynamic Models and Correlations for Bare and Wire-Wrapped Hexagonal Rod Bundles-Bundle Friction Factors, Subchannel Friction Factors and Mixing Parameters," Nuclear Engineering and Design, 92, 227 (1986).

25. F. E. Dunn and J. P. Herzog, "Thermal-Hydraulic Impact of Failure of Highly Irradiated Fuel Pins on LMR Passive Safety," Trans. Am. Nucl. Soc., 62, 673 (1990).

26. F. E. Dunn, R. A. Wigeland, and R. K. Lo, "RACS Shutdown Heat Removal in a Modular Sized LMR," Collected Papers in Heat Transfer 1988, Vol. II, ASME HTD-Vol. 104 pp. 211-215 (1988).

APPENDIX A

SUBROUTINES THAT WERE ADDED OR MODIFIED FOR THE MULTIPLE PIN MODEL

A number of new subroutines were written for the multiple pin model. In addition, modifications were made to a number of existing routines.

New Subroutines:

CHCHFL -- Calculates the subassembly-to-subassembly heat flux. Called at the beginning of each main time step.

HBSMPM -- Multiple pin version of HBSMPL. Calculates the fuel-to-cladding bond gap conductance if the simple model is used for this purpose.

SSCLM1 -- Called at the end of the null transient to set the initial coolant pressures and saturation temperatures. Also adjusts the orifices at the bottom of the pin section so that all channels in a subassembly have the same pin section pressure drop.

SSNULL -- Driver for the null transient.

TSCLM1 -- Transient coolant flow rate and pressure calculations for channels using the multiple-pin option.

TSHTM2 -- Multiple-pin version of TSHTN2. Transient temperatures in the gas plenum region.

TSHTM3 -- Multiple-pin version of TSHTN3. Transient temperatures in the core and axial blanket regions.

Modified Subroutines:

DTHFND -- Sets heat transfer time step size for a subassembly. Modified to account for the stability limit due to the use of explicit coolant convection in some channels if flow has reversed in some, but not all, channels.

POINST -- Modified to set the pointers used to access directly the channel data in the storage area.

SSINIT -- Modified to set all channel temperatures to the inlet temperature before the start of the null transient. Also calculates the initial value for the total subassembly flow if multiple channels are being used.

SSPRIM -- Modified to pick up the correct total subassembly coolant flow rate when setting the initial parameters for coupling with PRIMAR4.

SSTHRM -- Modified to include a call to SSNULL if the null transient is called for.

TSCLO -- Modified to call TSCLM1 if the multiple pin option is used.

TSCMPO -- Writes out data for plotting on unit 20. Modified to pick up and write out data for all channels used for a subassembly.

TSCNV3 -- Modified to use the correct coolant flow rate in the calculation of the coolant heat transfer coefficient.

TSHTN1, TSHTN2, TSHTN3 -- Modified to include subassembly-to-subassembly heat transfer by adding the heat flux from CHCHFL to the outer structure node.

TSHTN4 -- Modified to calculate the coolant heat transfer coefficient correctly when multiple-channels are used for a subassembly.

APPENDIX B

NEW INPUT FOR THE MULTIPLE PIN MODEL

Loc	Name	Meaning
87	ISSNUL	Number of time steps in the steady-state null transient for the core channels.
88	IPRSNL	Print out results every IPRSNL steps during the null transient.
		Block 11, OPCIN
88	DTNULL	Time step size for the steady-state null transient for the core channels.
		Block 51, INPCHN
205	NCHCH	Number of other channels that this channel is in contact with for duct wall-to-duct wall heat transfer. Maximum 8.
206-213	ICHCH (K)	Channel number of the Kth channel that this channel is in contact with. See also Bl. 63. loc. 82-89, HACHCH. If ICHCH > 1000, transfer heat from structure of ICH to coolant of ICHCH - 1000.
214	JJMLTP	Multiple pin option: 0 No multiple pin treatment for this subassembly. >0 This is the first of JJMLTP channels to represent the subassembly. <0 This is one of the additional channels use to represent the subassembly.
215-221	JMPIN	Reserved for later use by the multiple pin option.
284	IAXCON	0 No axial conduction in the coolant. 1 Axial conduction in the coolant. Not available if JJMLTP=0.
		Block 63, PMATCH
82-89	HACHCH	Channel-to-channel (duct wall-to-duct wall) heat transfer coefficient x area per unit length. Note: use the total duct wall contact area for all subassemblies involved.
104	TAUINV	Inverse of the heat transfer time constant. Used in computing the degree of implicitness for heat transfer calculations. Typical values: 5.0 for metal fuel 0.5 for oxide fuel

Block 64, COOLIN

189 UACH1
190 UACH2

Channel-to-channel heat flow at axial node j per pin in channel i per unit height from coolant in channel i to coolant in channel i+1 is calculated as:

$$Q(i,j)=(UACH1*k(j)+UACH2*c(j)*(w(i)+w(i+1))*(T(i,j)-T(i+1,j))$$

where

T (i,j) = coolant temperature
k = thermal conductivity of the coolant
c = coolant specific heat
w = coolant flow rate

k and c are calculated at the average of channel i and channel i+1 coolant temperatures.

Note: UACH1 and UACH2 are only used if JJMLTP.NE.0

Comments on Using the New Options

1. The multiple pin treatment only applies to the pin section. If a number of channels are used to represent a subassembly, the lower and upper reflector zones are only treated for the first of these channels. For the other channels, temperatures and coolant flow rates are only calculated in the pin section. This has a number of implications:
   (a) If channels F to L are used to represent concentric rings of pins in a subassembly, and if duct wall-to-duct-wall heat transfer is used for this subassembly, the channels should be numbered from the outside in. Channel F should represent the outer ring. and channel L should represent the inner ring. Otherwise, there will be no duct wall-to-duct wall heat transfer in the reflector zones.
   (b) In channel F, the coolant flow rate in the lower and upper zones is higher than in the pin section, since the total assembly flow in the reflector zones is represented by the one channel.
   (c) Some of the input variables for the reflector zones must be modified, rather than blindly using input from an old single channel per subassembly deck. If channel F represents n of the total m pins in the subassembly, then the coolant flow area per pin in a reflector zone is A_t/m, where A_t is the total area for the subassembly. Similarly, the structure and reflector perimeter per pin must be based on n pins in the reflector zones, and the orifice coefficients must be modified.

2. If either a multiple pin treatment or duct wall-to-duct wall heat transfer is being used, the old steady-state initialization for the temperatures will not give accurate results, since it ignores channel-to-channel heat transfer. In such cases, one should use the steady-state core channel null transient option (ISSNUL greater than zero and DTNULL greater than zero). In this case, the temperatures will all start at the inlet coolant plenum temperature. Then ISSNUL time steps of temperature calculations will be done for all channels, with the coolant flows held constant at their initial values. Coolant pressures are not calculated until the end of the null transient.

Distribution:

C. H. Adams
J. C. Braun
L. L. Briggs
F. B. Brown
J. E. Cahalan
F. E. Dunn (6)
E. E. Feldman
P. J. Finck
E. K. Fujita
P. L. Garner
E. M. Gelbard
K. C. Gross
J. P. Herzog
D. J. Hill
T. C. Hung
R. N. Hwang
Kalimullah
H. S. Khalil
J. Y. Ku
D. Mohr
Y. Orechwa
G. Palmiotti
P. A. Pizzica
R. H. Sevy
R. M. Singer
T. Sofu
A. M. Tentner
B. J. Toppel
R. B. Turski
R. B. Vilim
D. C. Wade
D. K. Warinner
A. M. White
R. A. Wigeland
B. S. Yarlagadda
J. F. Marchaterre
T. Y. Wei, RE
H. P. Planchon
RA Division Office (15)
J. Kopta

External Distribution for the ANL-FRA Report Series

Office of Isotope Production and Distribution, DOE-HQ, NE-48, GTN
Office of Technology Support Programs, DOE-HQ,NE-46, GTN
Office of Advanced Reactor Programs, DOE-HQ, NE-45, GTN
Nuclear Energy Facilities Operations & Testing Division, DOE-HQ, NE-472, GTN
LMR Division, DOE-HQ, NE-452, GTN
Advanced Technology Development Division, DOE-HQ, NE-462, GTN

D. T. Ingersoll, Leader, Nuclear Analysis & Shielding Section, ORNL
Division Leader, N-Division, LANL
A. E. Waltar, Manager, Safety and Control Technology, WHC (2)
Information Manager, Nuclear Safety Library, BNL (2)
Manager, Reactor Safety Research Department, Sandia (2)
R. S. Denning, Nuclear Facility Safety, Battelle Columbus
Manager, Safety Engineering, WARD (2)
Manager, LMFBR Physics and Safety, Rockwell International (2)
P. M. Magee, Manager, Design Analysis, GE (2)
EPRI LMFBR Group
Chief, Severe Accident Issues Branch, NRC/RES/SAIB (2)
Chief, Accident Evaluation Branch, NRC/RES/DSR
Executive Secretary, NRC-ACRS (5)

Information Services, Babcock & Wilcox Co.
X6 Group Leader, Mail Stop B226, Los Alamos National Laboratory
Manager, ARP Nuclear Engineering, Knolls Atomic Power Laboratory
M. Natelson, Manager, Reactor Technology, Bettis Atomic Power Laboratory
B. A. Worley, ORNL

C. Cowan, General Electric
M. Corradini, University of Wisconsin
J. W. Daughtry, Westinghouse Hanford Co.
P. W. Dickson, Westinghouse Savannah River Co.
R. Doncals, Westinghouse Electric Corp.
J. J. Dorning, University of Virginia
L. D. Felten, Rockwell International Corp.
N. C. Francis, Knolls Atomic Power Lab.
A. F. Henry, MIT
J. Kallfelz, Georgia Inst. of Tech.
T. S. Kress, ORNL
J. A. Lake, EG&G Idaho, Inc.
J. Lee, University of Michigan
E. Lewis, Northwestern University
M. R. Mendelson, Knolls Atomic Power Laboratory
W. F. Miller, Jr., ADRE, LANL
K. Ott, Purdue University
S. Pearlstein, Brookhaven National Laboratory
V. Ransom, Purdue University

DOE-OSTI (2)
ANL-W Library
ANL-E Library

ARGONNE
NATIONAL
LABORATORY

INTRA-LABORATORY MEMO

October 3, 1986

To: J. E. Cahalan

From: F. E. Dunn FED

Subject: SASSYS-1 Centrifugal Pump Model Validation

Introduction

Pump behavior during the coast-down after losing pump power, and the time at which the rotor locks are important factors in determining the transition from forced to natural circulation in liquid metal reactors (LMRs). This behavior is especially important when designing an inherently safe reactor[1,2] that will behave adequately even without active systems such as pony motors. Until prototype pumps for a new plant are built and tested, it is necessary to extrapolate pump behavior from older, existing pumps. Therefore, a homologous pump model has been implemented and tested against existing pump data for use in the design of new LMRs. This model has been implemented in both the SASSYS-1 code[3] and the COMMIX-1A code.[4] The predictions of this model agree with experimental data for the EBR-II pumps, the CRBR pumps, and the FFTF pumps, using the same basic homologous curves for pump head and hydraulic torque and using the same correlation for torque losses from shaft friction and windage for all three reactors.

The default parameters that were originally included in the SASSYS-1 homologous pump model did not match the head and torque curves given by Wylie and Streeter, [5,6] so the Wylie and Streeter curves were re-fit to obtain accurate correlations. The new fitting parameters are now the default parameters in SASSYS-1.

A locked rotor option was recently added to the homologous pump model. This option stops the rotor when the flow and rotor speed drop below user-specified values. After the rotor locks, the regular homologous correlation

is no longer used for pump head. Instead, a separate correlation is used for a locked-rotor.

II. Homologous Curves

In the dimensionless homologous pump theory of Wylie and Streeter[5,6], as modified by Marchal, Flesch, and Suter[7] the dimensionless head, $\bar{H}$, and hydraulic torque, $\bar{T}$, are evaluated as

$$\bar{H} = (\bar{N}^2 + \bar{Q}^2)W_h\ (x) \tag{1}$$

and

$$\bar{T} = (\bar{N}^2 + \bar{Q}^2)W_T(x) \tag{2}$$

where

$$x = \pi + \arctan\ (\bar{Q}/\bar{N}) \tag{3}$$

where $\bar{N}$ is the dimensionless speed (relative to the rated value), and $\bar{Q}$ is the relative volumetric flow rate. The functions $W_h(x)$ and $W_T(x)$ are given by Wylie and Streeter. For use in the SASSYS-1 code, the Wylie and Steeter values for a pump specific speed of 1800 gpm were fit using three-range sixth order polynomial fits, as indicated in Table 1. Note that the middle range (j=2) corresponds to the region of normal interest with $\bar{N} > 0$ and $\bar{Q} > 0$. This correlation agrees with the Wylie and Streeter curves to within .02 for W_h and within .04 for W_T. The table 1 values are now the default parameters in SASSYS-1. Single range 8th order polynominal fits have been used in COMMIX-1A.

Figures 1 and 2 show the Wylie and Streeter values for W_h and W_t, as well as the SASSYS-1 fits to these curves. Also shown are 8th order polynominal fits by Koenig for use in COMMIX-1A. The SASSYS-1 fits agree very well with Wylie and Streeter. The hoenig fits illustrate the problems encountered when trying to fit the whole range with a single polynominal. The fits usually used in COMMIX-1A are different fits that gain accuracy in the region of

interest (positive flow and positive rotor speed) by sacrificing accuracy in other regions.

The equation used for rotor speed, N, is

$$I \frac{dN}{dt} = T_m - T_r \bar{T} - T_r \bar{T}_\ell \tag{4}$$

where T_m is the motor torque, T_r is the rated hydraulic torque, and $\bar{T}_\ell$ is the normalized loss torque for bearing friction and windage, normalized to T_r. At normal operations speeds, the loss torque is small compared with the hydraulic torque, but at low speeds the loss torque dominates. Thus, the loss torque determines the shape of the flow coastdown tail and the time of rotor lock-up. Based on measurements on the CRBR pumps, Severson[8] came up with a correlation for $\bar{T}_\ell$ of the form

$$\bar{T}_\ell = \begin{cases} .01 - 73.13\,\bar{N}^2 & \text{if } .01 \geq \bar{N} \\ .00268 + .07\,\bar{N}^2 & \text{if } .268 \geq \bar{N} > .01 \\ .00383 + .01071\,\bar{N} + .01406\,\bar{N}^2 & \text{if } \bar{N} > .268 \end{cases} \tag{5}$$

III. Comparisons with Experimental Data

Figures 3 and 4 show comparisons between measured EBR-II pump data[9] and the Wylie and Streeter curves. Reasonable agreement is obtained.

The homologous pump model and the loss torque correlation of Eqn. 5 were used to calculate pump coast-downs for three pumps: EBR-II with a specific speed of 28.1 (1450 gpm), FFTF with a specific speed of 24.48 (1264 gpm), and CRBR with a specific speed of 40.08 (2069 gpm). The calculations for FFTF acceptance tests[10] and the CRBR calculations were done by D. Malloy with COMIX-1A, and the calculations for the EBR-II SHRT-19 test[12] were done with SASSYS-1. In all cases, the model calculations agree reasonably well with experimental measurements. Figure 5 shows the agreement for EBR-II.

In summary, a single set of homologous pump characteristic curves and a single torque loss correlation were found to be adequate to predict the

coastdown behavior of the EBR-II, FFTF, and CRBR pumps. These comparisons essentially validate the contention that homologous pump methodology is an accurate representation for typical centrifugal pumps. It was also demonstrated that the frictional torque expression largely determines the rotor lock time. The above CRBR pump expression has been used successfully on other pumps; however, its general applicability is not guaranteed.

IV. Locked-Rotor Option

A locked-rotor option has been added to the homologous pump model in SASSYS-1. If the normalized flow through a pump drops below a user-spcified value and if the normalized rotor speed drops below another user-specified value then the rotor locks. After the rotor locks, the normalized pump head is calculated as

$$\bar{H} = \begin{cases} -C_1 \bar{W}^2 & \text{if } \bar{W} \geq \bar{W}_T \\ -C_1 \bar{W}_T \bar{W} & \text{if } \bar{W} < \bar{W}_T \end{cases} \qquad (6)$$

where $\bar{W}$ is the normalized mass flow rate, and $\bar{W}_T$ is a transition flow rate for the transition from turbulent to laminar flow.

V. Using the Homologous Pump Model

The current version of the homologous pump model is in members SSPUMP, PUMPFL and PUMPFN Of data set B18175.SAS4A.MAY86.LOAD.

Much of the input for the homologous pump model (IEMPMP(IPMP)=2) is the same as for the older centrifugal pump model (IEMPMP(IPMP)=1). One large difference is in the meaning of the variable ADMPHD(K,IPMP). Table 2 lists the meaning of a APMPHD for the homologous pump model.

Distribution:

J. F. Marchaterre
Y. I. Chang
A. J. Goldman
D. R. Pedersen
R. H. Sevy
P. A. Pizzica
H. H. Hummel
Accident Analysis Section

Table 1. Coefficients for Fits to Wylie and Streeter Pump Head and Torque Curves

$$W_h(x) = \sum_{i=0}^{6} a_{hji}\, x^i \qquad W_T(x) = \sum_{i=0}^{6} a_{Tji}\, x^i$$

	j=1, $\pi > x \geq 0$		j=2, $3\pi/2 \geq x \geq \pi$		j=3, $2\pi > x > 3\pi/2$	
i	a_h	a_T	a_h	a_T	a_h	a_T
0	.63380980	-.68436766	431.96699	-1154.9471	6171.9821	-379.81080
1	.46015764	2.7759909	-576.61438	1858.4915	-4958.9692	726.14914
2	-2.40040490	-5.3988010	301.00029	-1237.6683	1406.3329	-496.25029
3	3.17937240	6.8541205	-75.465856	436.01653	-126.17344	167.64136
4	-1.77304490	-4.0757860	8.6754986	-85.573772	-13.217121	-30.366923
5	.46235776	1.0813311	-.26062352	8.8627717	3.2450530	2.8311896
6	-.04624640	-.10475812	-.01596287	-.37830487	-.16925040	-.10681625

Table 2. Meaning of APMPHD(K,IPMP) for the Homologous Pump Model

K	Meaning	Suggested Value
1	torque loss coefficients, low range, $\bar{S}$ APMPHD(10,IPMP)	0.01
2		0
3		73.13
4	torque loss coefficients, middle range APMPHD(11,IPMP) $\bar{S}$ > APMPHD(10,IPMP)	.00268
5		0.
6		.07
7	torque loss coefficients, high range $\bar{S}$ > APMPHD(11,IPMP)	.00383
8		.01071
9		.01406
10	limits of torque loss ranges	.01
11		.268
12	coefficient C_1 in locked rotor pressure drop	
13	transition $\bar{W}_T$, laminar to turbulent	
14	unused	
15	unused	
16	unused	
17	unused	
18	L, pump curve number (1, 2, or 3)	1
19	$\bar{W}$for locked-rotor	.03
20	$\bar{S}$for locked rotor	.03

References

1. J. E. Cahalan, R. H. Sevy, and S. F. Su, "Accomodation of Unprotected Accidents by Inherent Safety Design Features in Metallic and Oxide-Fueled LMFBRs," Proc. Intl. Topical Mtg. Fast Reactor Safety, Knoxville, TN (1985) pp. 29-33.

2. R. T. Lancet and J. F. Marchaterre, "Inherent Safety of the SAFR Plant," Proc. Intl. Topical Mtg. Fast Reactor Safety, Knoxville, TN (1985) pp. 43-49.

3. F. E. Dunn, F. G. Prohammer, and D. P. Weber, "The SASSYS-1 LMFBR Systems Analysis Code," Proc. Intl. Topical Mtg. Fast Reactor Safety, Knoxville, TN (1985) pp. 949-1006.

4. H. M. Domanus, R. E. Schmitt, W. T. Sha, and V. L. Shah, "COMMIX-1A: A Three-Dimensional Transient Single-Phase Computer Program for Thermal Hydraulic Analysis of Single and Multicomponent Systems" NUREG/CR-2896 (1983).

5. E. B. Wylie and V. L. Streeter, Hydraulic Transients; Chapter Nine, McGraw-Hill, New York, 1967.

6. E. B. Wylie and V. L. Streeter, Fluid Transients; Chapter Six, McGraw-Hill, New York, 1978.

7. M. Marchal, G. Flesch, and P. Suter, "The Calculation of Waterhammer Problems by Means of the Digital Computer," Proc. Int. Symp. Waterhammer Pumped Storage Projects, ASME, Chicago, Illinois, November 1965.

8. W. J. Severson et al., personal communication, February 1982.

9. EBR-II System Design Descriptions, Volume II Primary System, Chapter 3 Primary Cooling System, p. 3.5-18.

10. H. P. Planchon, et al., personal communication, August 1979.

11. D. J. Malloy, "A Homologous Pump Model for LMR Transient Calculations," FRA-TM-151 (May, 1985).

12. H. P. Planchon, et al., "The Experimental Breeder Reactor II Inherent Shutdown and Heat Removal Tests - Results and Analysis," Proc. Intl. Topical Mtg. Fast Reactor Safety, Knoxville, TN (1985) pp. 281-291.

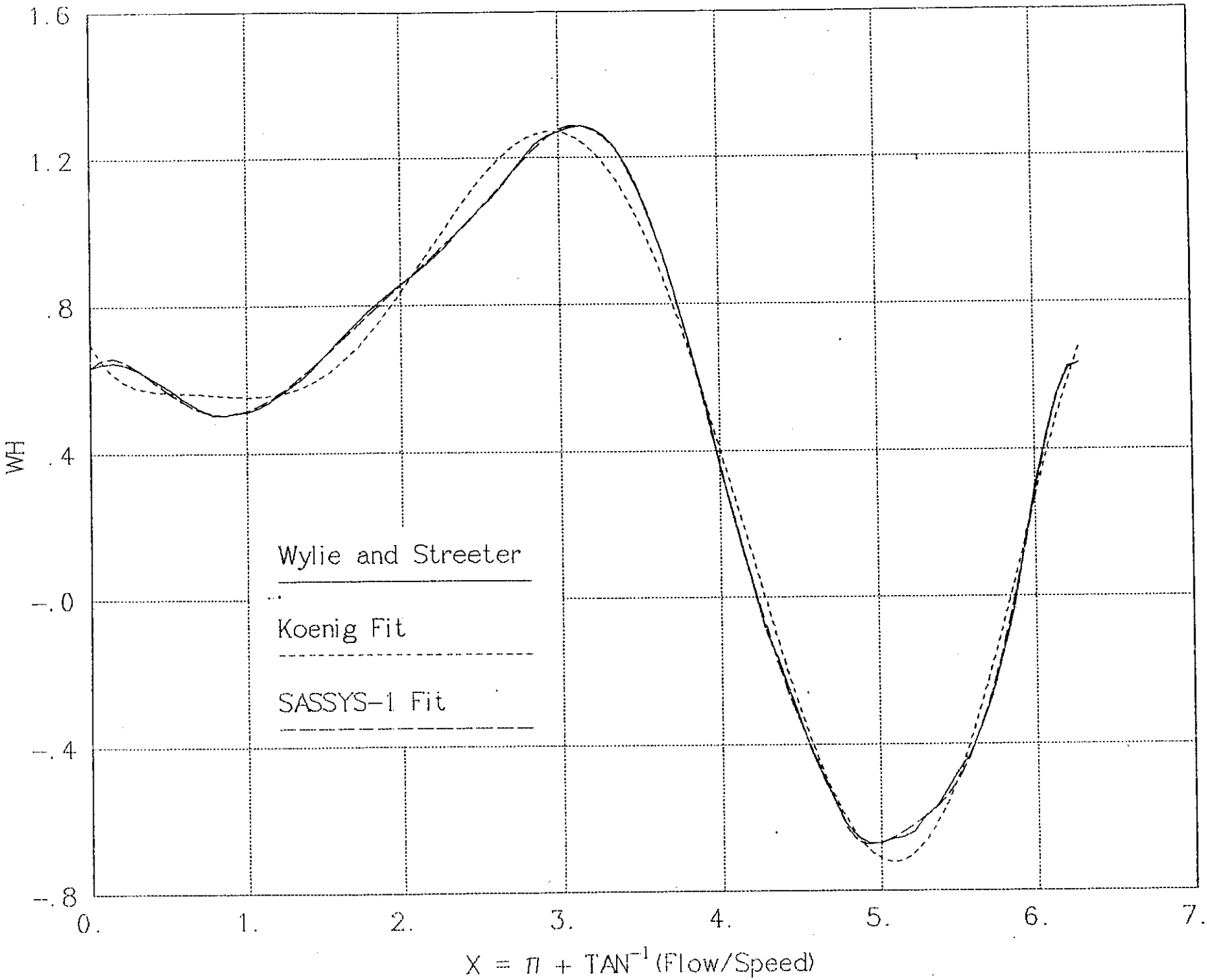

Fig. 1. Dynamic Head, Data and Fits

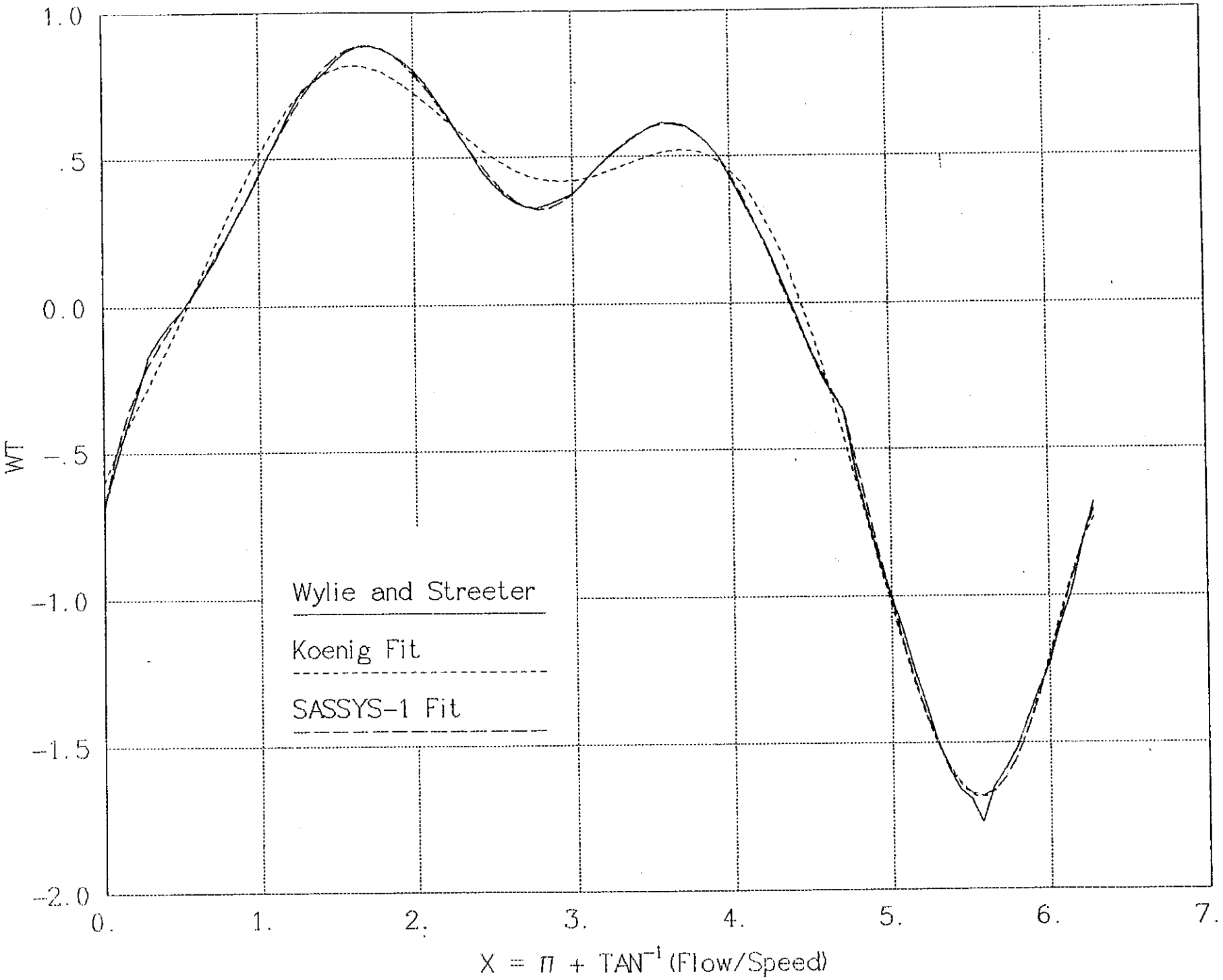

Fig. 2. Hydraulic Torque, Data and Fits

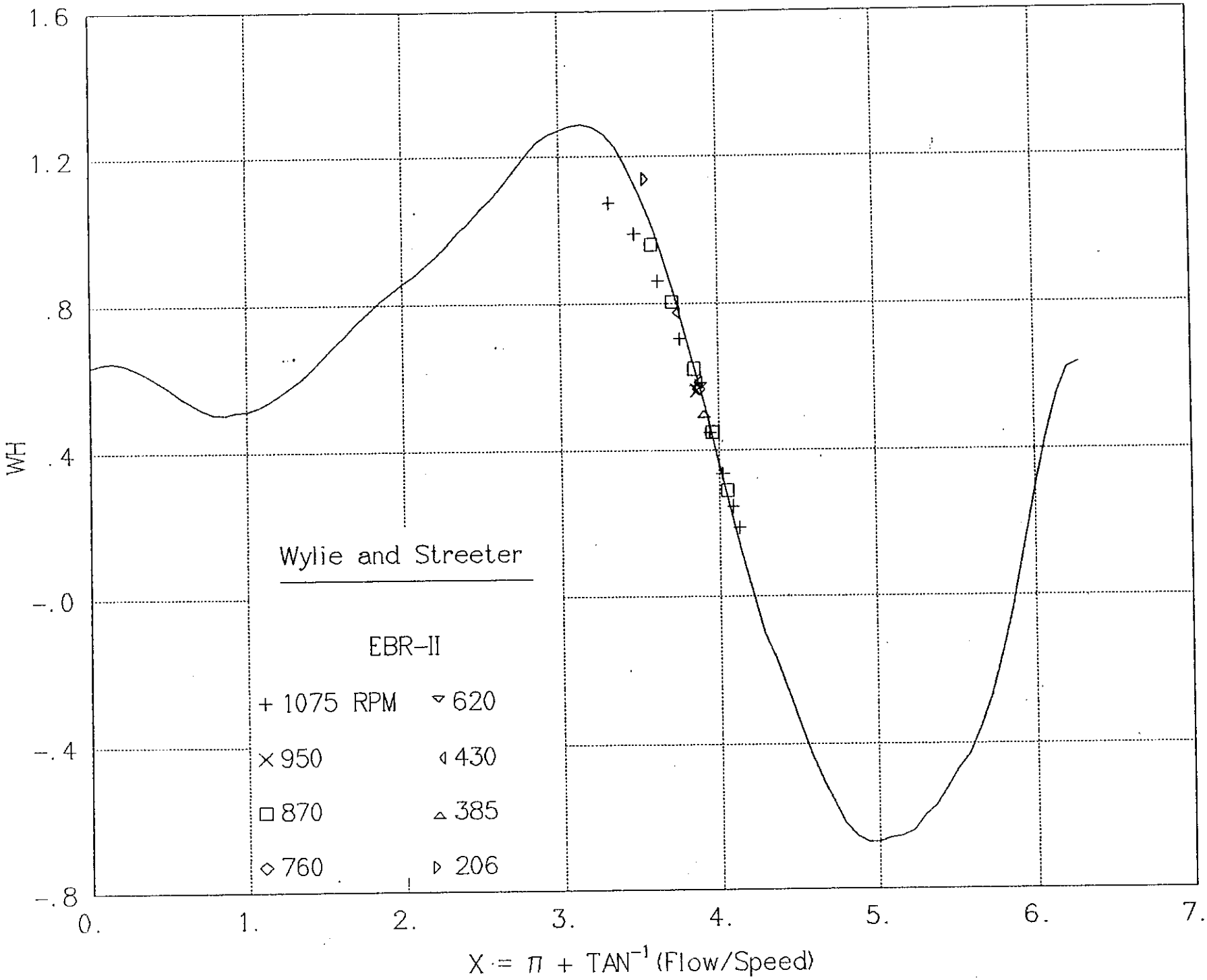

Fig. 3. Dynamic Head, EBR-II Data

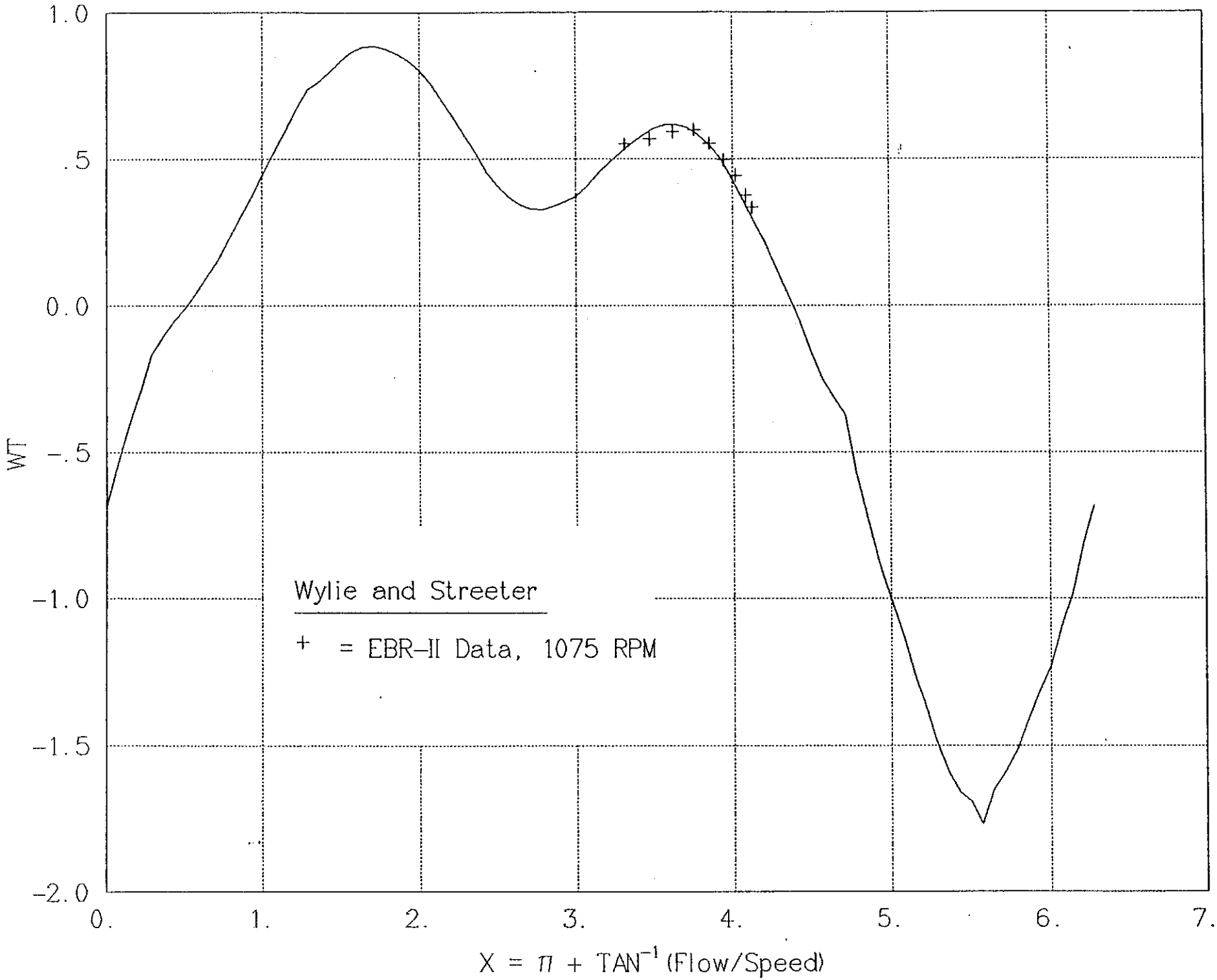

Fig. 4. Hydraulic Torque, EBR-II Data

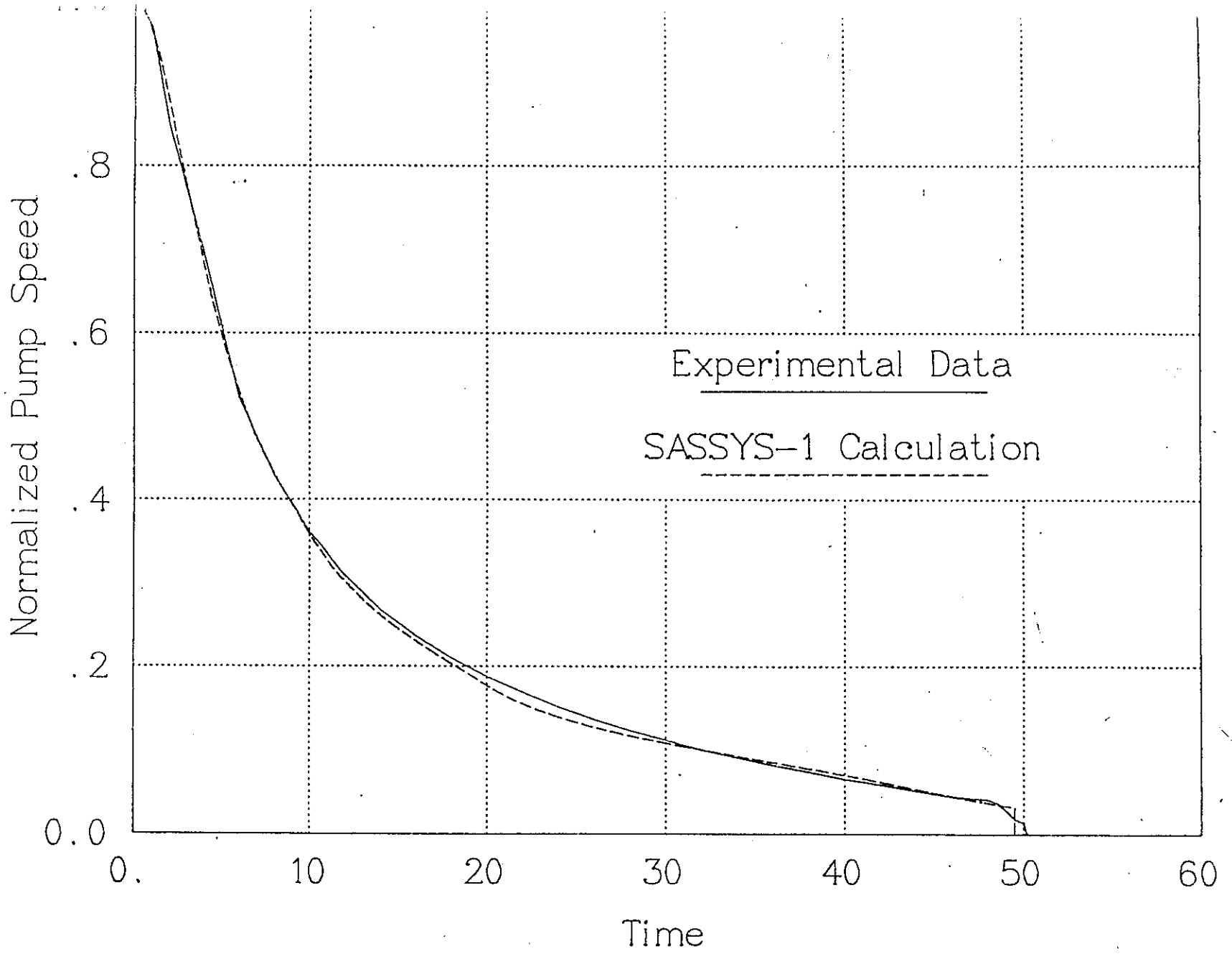

Fig. 5. EBR-II Pump Speed, SHRT-17 Test